Calpain DEK1 acts as a developmental switch gatekeeping cell fate transitions

Viktor Demko[1,5], Tatiana Belova[1,6], Maxim Messerer[2], Torgeir R. Hvidsten[3], Pierre-François Perroud[4], Klaus F.X. Mayer[2,7], Odd-Arne Olsen[1], Daniel Lang[2]*

1 Department of Plant Sciences, Norwegian University of Life Sciences, P.O.Box 5003, NO-1432 Ås, Norway
2 Plant Genome and Systems Biology, Helmholtz Center Munich - Research Center for Environmental Health, 85764 Neuherberg, Germany
3 Faculty of Chemistry, Biotechnology and Food Science, Norwegian University of Life Sciences, Ås, Norway
4 Institut Jean-Pierre Bourgin, INRAE, AgroParisTech, Université Paris-Saclay, 78000 Versailles, France
5 Current address: Department of Plant Physiology, Faculty of Natural Sciences, Comenius University in Bratislava, Ilkovicova 6, 84104 Bratislava, Slovakia; Plant Science and Biodiversity Center, Slovak Academy of Sciences, Dubravska cesta 9, 84104 Bratislava, Slovakia.
6 Current address: Centre for Molecular Medicine Norway, University of Oslo, Oslo, Norway
7 School of Life Sciences, Technical University Munich, 85354 Freising, Germany

Contact info

* Corresponding author daniel.lang@mailbox.org

Summary

Calpains are cysteine proteases that control cell fate transitions. Although calpains are viewed as modulatory proteases displaying severe, pleiotropic phenotypes in eukaryotes, human calpain targets are also directed to the N-end rule degradatory pathway. Several of these destabilized targets are transcription factors, hinting at a gene regulatory role. Here, we analyze the gene regulatory networks of *Physcomitrium patens* and characterize the regulons that are deregulated in DEK1 calpain mutants. Predicted cleavage patterns of regulatory hierarchies in the five DEK1-controlled subnetworks are consistent with the gene's pleiotropy and the regulatory role in cell fate transitions targeting a broad spectrum of functions. Network structure suggests DEK1-gated sequential transition between cell fates in 2D to 3D development. We anticipate that both our method combining phenotyping, transcriptomics and data science to dissect phenotypic traits and our model explaining the calpain's role as a switch gatekeeping cell fate transitions will inform biology beyond plant development.

Keywords

Cell fate transitions, DEK1 calpain, gene regulatory network analysis, N-end rule degradatory pathway, pleiotropy, developmental switch, land plant regulons, genotype-phenotype mapping, Physcomitrella, *Physcomitrium patens*

Introduction

Multicellular organisms are dependent on the establishment of distinct cellular identities to implement individual tissues, cell types and functions. In the course of development, cells acquire specific cellular fates resulting in either division, differentiation or death. A cell fate is the product of a specific expression state, leading to a distinct cellular complement of RNAs and proteins that provide a specific competence to respond to environmental signals and developmental patterning cues (Pierre-Jerome et al., 2018; Casey et al., 2020). The transition between different cellular fates requires both the reprogramming of the gene expression state as well as the modulation or exchange of the cell's protein complement. In many instances, cell fate transitions are the result of asymmetric cell division. In plants, cell fate is dependent on spatial localization and intercellular communication via direct protein-protein interactions or mobile signals like phytohormones, peptides or transcription factors (Pierre-Jerome et al., 2018; Gundu et al., 2020; Hata and Kyozuka, 2021). This process must be highly coordinated in order to synchronously implement the changes on an epigenetic, transcriptional, post-transcriptional, translational and post-translational level.

Asymmetric, formative cell divisions mostly involve a reorientation of the division plane and depend on both intrinsic and extrinsic factors (Shao and Dong, 2016; de Keijzer et al., 2021). This divisional asymmetry requires direct modification or exchange of cytoskeletal components or other proteins and protein complexes affecting cell polarity. Thus, plant cell fate transitions depend on pathways implementing the physical asymmetry of cell division as well as the regulatory (re)programming of divergent cellular identities. Dependence on positional and other extrinsic signals necessitates the tight integration of all physical and regulatory layers determining plant cell fate. How are the different physical and regulatory layers coordinated and synchronized to a new cell fate and how is the integration of potentially conflicting extrinsic signals and intrinsic factors implemented?

The endosperm aleurone as well as the protodermal or the derived epidermal L1 layers of flowering plants are prime examples for cell fate specifications that depend on these processes. Both cell types implement the outer layers of the respective flowering plant tissues, emerge by asymmetric cell division and are specified by positional information (Takada and Iida, 2014; Olsen, 2020). Remarkably, these cell fate specifications fail in deletion or loss of function mutants of the DEFECTIVE KERNEL 1 (DEK1) gene in mono- (Becraft et al., 2002; Lid et al., 2002) and dicotyledonous (Lid et al., 2005; Johnson et al., 2005) plants. The failed embryonal cell fate transition has tremendous impact on further plant development - it is arrested at the globular embryo stage, because the L1 layer is crucial to the regulation of shoot stem cell maintenance and organ growth (Takada and Iida, 2014). DEK1 mutants in various organisms display pleiotropic phenotypes and are always severely impeded in further development (Ahn et al., 2004; Lid et al., 2005; Hibara et al., 2009; Liang et al., 2015; Amanda et al., 2017). DEK1 is essential for flowering plant seed, embryo, epidermis, trichome, leaf and shoot apical meristem development (Olsen et al., 2015). Consistent with the assessment of DEK1 as one of the key components in land plant meristem evolution (Harrison, 2015), studies in the bryophyte model system

Physcomitrium patens (Physcomitrella; Rensing et al., 2020) demonstrated a vital role as a developmental regulator controlling cell fate decisions in the moss' simplex meristems involved in the 2D to 3D transition (Perroud et al., 2014; Demko et al., 2014).

At the molecular level, DEK1 seems to affect both physical and regulatory layers governing cell fate transitions. In terms of the physical, asymmetry determining factors, DEK1 null mutants display disorganization of division planes resulting in defective division patterns and cell shapes (Lid et al., 2005; Perroud et al., 2014). These phenotypes are caused by defects in microtubule-organized orientation (Liang et al., 2015), the deposition and remodeling of the cell wall as well as cell adhesion (Amanda et al., 2016). Changes in gene expression levels and patterns hint towards a role also in the regulatory layers. These comprise the deregulation of several cell type-specific markers like the HD-ZIP family IV transcription factors (TFs: ML1, PDF2, HDG11, HDG12, and HDG2; Galletti et al., 2015), as well as other embryo- and post-embryo developmental regulators (e.g. CLV3, STM, WOX2, WUS, PIN4; Liang et al., 2015) and potential downstream target genes involved in cell wall biosynthesis and remodeling and similar functions related to the differentiation of the respective cell type (XTH19, XTH31, PME35, GAUT1, CGR2, EXP11; Amanda et al., 2016; Amanda et al., 2017).

DEK1 is a 240 kDa multi-pass transmembrane (TM) protein with a cytosolic calpain cysteine protease (*CysPc* and *C2L* domains) as the effector (Fig. 1a). Other structural features include a long cytosolic *loop* region between TM domain 9 and 10 as well as an *LG3*-like region in the cytosolic *linker* connecting the membrane domain (*MEM*) with the calpain protease domain (*CysPc-C2L;* Demko et al., 2014; Johansen et al., 2016). The DEK1 calpains or TML-calpains comprise a subfamily of a deeply conserved, multi-domain superfamily of calpains sharing a common *CysPc* domain that likely evolved in eubacteria (Zhao et al., 2012). The clade of the animal-specific, so-called classical calpains are mechanistically the best characterized and have been described as the third proteolytic system besides the lysosomal and proteasomal systems (Spinozzi et al., 2021). Contrary to the latter two degradatory systems, the Ca^{2+}-dependent calpains are modulatory proteases that cleave proteins at a limited number of specific sites, generating fragments or neo-proteins with novel functions (Zhao et al., 2012; Cardoso et al., 2019). These e.g. comprise maturation from an inactive preprotein, modulation of stability and association of multiprotein complexes or modification of subcellular localizations. Like plant DEK1 calpains, classical calpains are pivotal to animal development and cell fate transitions with roles in early embryonic patterning, muscle and neural development and homeostasis, cell migration, Wnt signalling during tissue morphogenesis and axial patterning via the NFκB/IκB pathway (Araujo et al., 2018). The functional roles in the regulation of cell division and the cell cycle seems to be the ancestral state of the entire superfamily (Zhao et al., 2012; Vieira et al., 2017). Consistent with the broad functional importance of the calpain system as well as the pleiotropy and severity of loss of function mutants in various eukaryotic model systems, human calpains have been found as aggravating factors in many pathophysiological conditions and illnesses including various cancers and hereditary diseases like muscular dystrophy (Storr et al., 2011; Ono and Sorimachi, 2012; Ono et al., 2016; Araujo et al., 2018).

The *CysPc-C2L* protease domain of DEK1 calpains is functionally conserved among land plants (Liang et al., 2013). It comprises the catalytic sites also found in the classical calpains and is a functional cysteine protease (Wang et al., 2003). Although its catalytic activity does not seem to depend on Ca^{2+} *in vitro,* it is increased in the presence of mM Ca^{2+} levels (Wang et al., 2003). Like classical calpains, the full DEK1 protein demonstrates autoproteolytic activity releasing several soluble neo-proteins with cytosolic localization (Johnson et al., 2008). The membrane-localized full-length protein thus likely represents the inactive calpain that might be activated by phosphorylation (Moody, 2019), mechanosensing (Tran et al., 2017) or other sources emitting local Ca^{2+} pulses similar to the classical calpains (Araujo et a., 2018). All of this, taken together with the phylogeny, phenotypic data and the observed broad functionality that is expressed by conserved functions in basic biological processes and convergently evolved roles in development, points to a deep conservation of the *CysPc-C2L* protease domain's molecular function. The alternate domain architectures of the superfamily evolved by domain shuffling and likely accommodate independent, but convergent ways to modulate, specify or restrict the catalytic activity of the calpain protease (Zhao et al., 2012).

Calpains display a fuzzy target specificity that is less reliant on the primary sequence of the substrate and possibly depends on higher order factors like 2D/3D protein structure or cofactors (Ono and Sorimachi, 2012; Araujo et al., 2018). Coupled with the modulatory role of the protease and the broadness of the involved biological processes, the seeming lack of specificity has been a limiting factor for the mechanistic exploration and systematic identification of calpain targets (Ono et al., 2016). As a result, so far there are a few hundred confirmed calpain substrates, most of which have been reported in mammals. In plants, so far no direct substrates of the DEK1 calpain have been identified. Generally, it has been extremely difficult to mechanistically align the view of a non-degradatory, modulatory but relatively unspecific protease with the diversity, ubiquity, severity and impact of calpain defects and mutations.

In vitro and *in vivo* degradation assays of confirmed mammalian calpain targets (Piatkov et al., 2014) revealed them as short-lived substrates for the N-end rule degradation or N-degron pathway (NERD; Majovsky et al., 2014; Nguyen et al., 2018; Holdsworth et al., 2020). Natural C-terminal fragments of a variety of mammalian proteins, including transcriptional regulators, bear N-terminal residues, so-called N-degrons, that attract and activate the components of the NERD pathway and ultimately lead to their degradation by the ubiquitin-proteasome system (Piatkov et al., 2014). This also explains the short half-life of auto-proteolytic cleavages in mouse and fruit fly calpains resulting in N-degron fragments (Farkas et al., 2004; Piatkov et al., 2014). Thus, in these instances calpain cleavage leads to destabilization or inhibition of biological functions, providing a plausible explanation to align the limited target specificity with the broad biological impact of the cysteine proteases.

Considering that the targets of such cleavages also comprise TFs and other transcriptional regulators, a more direct route to the control of both the physical and regulatory layers of cell fate transitions emerges. In this case, calpains act as post-translational regulators of gene functions either a) by directly modulating the proteins' function, b) by indirectly affecting the target protein's stability marking them

for the NERD pathway or c) by indirectly controlling the stability of the gene's transcriptional regulators (Fig. 1e). While a) represents a positive control over a gene's function, b) an inhibitory, negative control, the outcome of c) depends on whether the targeted TF or regulator represents a transcriptional activator or repressor and thus allows a bidirectional control of gene functions.

Due to its subcellular localization in the plasma membrane and its role in the establishment of cell division plane orientation, so far studies of the plant calpain have been designed with a scenario in mind where DEK1 only acts as a modulatory protease (a) targeting a limited number of specific targets e.g. in or around the cell division plane apparatus. Combining the pleiotropy and developmental essentiality in DEK1 mutants, the fuzzy target specificity and the broad range of functions with the inhibitory role in targeting proteins to the NERD pathway, we postulate a second scenario (*dual role scenario*): the calpain directly modulates specific protein functions (a) and indirectly controls the half-life of potentially many proteins (b). These include transcriptional regulators and thereby affect the expression of a large number of target genes (c).

The model moss *P. patens* provides an ideal system to evaluate these two scenarios. Generally, its evolutionary position as a representative of the earliest diverging clade of land plants, the available reference genome and high-quality annotation resources (Lang et al., 2018), the well-established molecular toolbox and the comprehensive transcriptomics resources covering the entire life cycle (e.g. Frank and Scanlon, 2015; Perroud et al., 2018; Kirbis et al., 2020) make it an attractive model of choice for land plant evo-devo studies like ours (Rensing et al, 2020; Hata and Kyozuka, 2021; Keijzer et al., 2021). Specifically, the simple morphological structures in the early development of the moss, comprising mostly single-cell-layered tissues, is not impeded in the DEK1 null mutants (Perroud et al., 2014; Demko et al., 2014; Johansen et al., 2016) and thus facilitate transcriptional and phenotypic profiling along a longer developmental time course including the 2D to 3D transition of the moss' simplex shoot meristem. The NERD pathway is conserved among land plants and *P. patens* is ideally suited to assess the calpain's potential role as a post-translation gene regulator feeding into this pathway, because mutants of the moss' NERD pathway display a phenotype that is highly similar to DEK1 (Hoernstein et al., 2016; Schuessele et al., 2016).

We set out to elucidate DEK1's role in plant development and gene regulation by combining phenotypic and transcriptional profiling of wild-type and mutant moss lines with a comprehensive, genome-wide, integrative, multi-scale data mining approach to analyze the mutant deregulation profiles of the global gene regulatory networks. Our analysis sheds light on the molecular nature underlying the pleiotropic developmental phenotypes caused by DEK1. The predicted gene regulatory network allows to connect the calpain's biochemical function and regulatory consequences supporting its role as a post-translational gene regulator. We combined phenotyping, transcriptomics and data science to dissect phenotypic traits. The annotated, genome-wide gene regulatory network is a valuable resource facilitating next generation plant evo-devo research. The proposed model gives insights into the calpain's role as a developmental switch gatekeeping cell fate transitions.

Results

DEK1 dramatically impacts moss development

Previous work demonstrated that mutations in the DEK1 gene dramatically affect *P. patens* development (Olsen et al., 2015). Here, we characterize and quantify phenotypes and global gene expression profiles of five moss lines. In addition to wild-type (WT), a *Δdek1* deletion strain (Perroud et al., 2014), a strain overexpressing the DEK1 linker and calpain domains (Fig. 1a) under the maize ubiquitin promoter (*oex1*) and two partial domain-deletion lines, *Δloop* (Demko et at., 2014) and *Δlg3* (Johansen et al., 2016), were studied (Fig.1a). These lines were sampled at five time points that comprise the early and intermediate stages of *P. patens* development, including the transition from 2D tip-growth in the filamentous protonema to 3D apical growth in leafy shoots (gametophores; Fig. 1b). While the early stages of protonema development are largely unaltered in the *Δdek1* and *Δloop* mutants (Fig. 1b), the later stages as well as the formation of gametophores are significantly disturbed in all mutant strains.

Comparison of the developmental defects in the deletion and overexpression lines, highlights systematic, diametrically opposing effects of the two mutation types as compared to WT. These diametrical phenotypes include reduced (*Δdek1*) vs. enhanced (*oex1*) secondary filament extension, higher vs. lower percentage of filaments that form buds (*Δdek1*/*oex1*) and a four times higher gametophore bud initiation rate per filament in *Δdek1* (Fig. 1b,c).

The partial *Δloop* deletion line shows milder phenotypic changes than *Δdek1*, except for bud development which, instead of stopping, continues to proliferate forming naked stems without initiation of phyllids. *Δlg3* displays unique phenotypes including severely affected protonema differentiation and branching resulting in reduced plant size, as well as aberrant gametophore formation. Juvenile *Δlg3* plants display stunted phyllids.

How can altering one membrane-bound protease have such variable, complex and drastic effects on plant development? The clear, diametrical behaviour of the deletion and overexpression lines, as well as the intermediate phenotypes of the partial deletions, provide the opportunity to shed light into this question by evaluating the global, molecular consequences of DEK1 mutation using differential transcriptomics.

Many genes and functions are deregulated in DEK1 mutants

We performed differential gene expression (DGE) analysis based on triplicate RNAseq libraries generated for the developmental time course described above. Expression levels for all non-redundant transcripts of protein- and non-protein coding genes were quantified, condensed per gene and subsequently tested for DGE along the time course using kallisto/sleuth (Bray et al., 2016; Pimentel et al., 2017). Sets of up- and down-regulated genes in the mutants were identified at 10% FDR (Fig 1d; see Supplementary Table ST1 for statistics with FDR 10% and 1%). The impact of DEK1 mutation on overall gene regulation can be defined as the total sum of differentially expressed or up- and down-regulated genes, i.e. the total number of deregulated genes in each mutant line. Consistent with

the dramatic phenotypic consequences in *Δdek1*, *oex1*, *Δloop* and *Δlg3*, the DGE analysis revealed a substantial number of deregulated genes in the mutants. The largest number of deregulated genes is observed in the *Δdek1* (35% of all genes) and *oex1* (44% in comparison to wild type and 49% relative to *Δdek1* levels) lines. Whereas in the partial deletion lines *Δloop* and *Δlg3* about 7% of all genes are deregulated. Overall, we observe balanced directionality of deregulation in all studied contrasts, i.e. similar number of up and down-regulated genes.

Overall, the extent of deregulated genes supports a scenario where the DEK1 calpain controls the half life of transcriptional regulators and thereby indirectly affects the expression of a large number of target genes (*dual role scenario*). This also allows us to explain the observed balanced directionality of deregulated genes that is consistent with a uniform distribution of direct DEK1 cleavage targets, comprising equal proportions of gene activators and repressors. The lack of a few, specific, modulatory calpain cleavages alone unlikely leads to such pronounced transcriptional changes. Such specific action likely would result in only specific functions to be deregulated. To delineate the functional consequences of mutating DEK1, we utilized Gene and Plant Ontology annotations to assess the percentages of terms and genes that are deregulated in the mutants (Fig. SF1; Table ST2). Consistent with a broad target prevalence of DEK1 (*dual role scenario*) and the observed complex, pleiotropic phenotype, the analysis demonstrates that 85% of molecular functions, 88% of biological processes, 90% of cellular components, 92% anatomical entities and 94% of all developmental stages in GO and PO are deregulated in *Δdek1*.

Potential indirect DEK1 targets display consistent mutant deregulation patterns

Given the *dual role scenario*, DEK1 acts as a post-translational regulator (Fig. 1e) of ubiquitous gene functions. This should be reflected in the global expression patterns of the mutants: Down-stream genes of repressors that are cleaved by DEK1 at the protein-level, will be up-regulated in the over-expressor and down-regulated in the null mutant (referred to as *repressor targets* below). Down-stream genes of DEK1-controlled activators should respond in a diametrically opposite fashion (*activator targets*).

To assess this, we performed multiple set analysis of the differentially expressed genes to identify dominant deregulation patterns (Fig. 1f). Indeed, the two top emerging patterns comprise consistently deregulated, diametrically responding genes. The largest set (red bar; Fig. 1f) comprises 2,639 genes which are down-regulated in *Δdek1* and up-regulated in *oex1*. This profile is consistent with the hypothesis that these genes are targets of DEK1-controlled repressors (Fig. 1e). The second largest set (blue bar; Fig. 1f) comprises 2,445 genes that are up-regulated in *Δdek1* and down-regulated in *oex1*. These genes are potentially controlled by DEK1-targeted activators (Fig. 1e). The third and fourth most frequent patterns are subsets of these two patterns. Both gene sets also likely comprise indirect targets of DEK1. Thus, the dominant, global expression patterns of deregulated genes are in line with the *dual role scenario* and all of these deregulated genes can be considered as indirect DEK1 targets. In the subsequent analyses, we focused on the two major sets of consistently deregulated genes as potential indirect DEK1 *repressor* and *activator targets* (Fig. 1f).

During wild type gametophyte development 71% and 75% of the putative DEK1-controlled *repressor* and *activator targets* respectively display significant expression level changes. The two sets substantially differ in their expression patterns along the time course. For example, while 765 of the *repressor targets* are more active during the early phase (days 3-5, Fig. 1b), 794 of the *activator targets* are up-regulated during the later phases of development (days 9-14). This might indicate that some of these potential DEK1-targets are involved in the developmental transitions occurring during this time interval. Taken together, the evidence from the deregulated transcriptomes of DEK1 mutants and the wild type is consistent with the role of the plant calpain acting as a post-translational regulator with a broad range of direct or indirect targets and encoded gene functions whose timed expression is consistent with the observed, severe and pleiotropic mutant phenotype.

5 out of 11 GRN subnetworks are enriched for putative DEK1 targets

To further evaluate the *dual role scenario*, we set out to look for patterns of consistent deregulation in the moss' gene regulatory networks (GRNs). As a basis, we predicted genome-wide regulatory interactions based on 374 paired RNASeq libraries and 1,736 regulators using the Random Forest predictor of GENIE3 (Huynh-Thu et al., 2010). The overall directionality of the regulatory interactions, i.e. positive (activating) or negative (repressive) regulation, was determined by the correlation coefficient of regulator and target gene expression levels along the developmental time course. Subsequent community detection of the top10 regulatory interactions for 35,706 genes resulted in 11 robust subnetworks (Fig. SF2a). We subsequently utilized the predicted regulatory interactions and subnetworks as tools to assess the putative gene regulatory role of DEK1.

We employed network enrichment analysis of candidate gene sets inferred from the DGE analyses in the subnetwork graphs (Signorelli et al., 2016). This revealed significant enrichment of regulatory relationships for DEK1-controlled *repressor* and *activator targets* in subnetworks II, V VIII, IX and X (FDR<<0.01; rows 1 and 3 of Fig. 2a; Fig. SF2b). Based on peak activities of gene expression during wild type gametophyte development, subnetwork V is enriched for *repressor targets* active during the early phase comprising mostly chloronema filaments (3-5d; row 2 Fig. 2a). Subnetworks II and X are enriched for *activator targets* which are expressed during the 2D to 3D transition (9-14d; row 5 Fig. 2a). By tracing the regulatory links of deregulated genes, the GRN allowed us to identify upstream TFs representing potential direct cleavage targets of the DEK1 calpain with unaffected expression in the mutants. Consequently, we tested subnetworks for enrichment of such upstream TFs predicted to directly control any of the deregulated genes. While this analysis again highlighted subnetworks II, VIII, and X, it also suggested potential direct cleavage targets in three other subnetworks (I, III and XI; row 4 in Fig. 2a). As the deregulated targets of these TFs predominantly also fall in the five DEK1-controlled subnetworks, the latter group of regulators might serve as DEK1-controlled interfaces to other regulatory circuits.

Jointly these analyses suggest that the set of DEK1-deregulated genes can be traced to five predominantly enriched subnetworks. Fig. 2b depicts the overall network structure of the putative indirect DEK1 targets (color-coded by deregulation pattern) including direct upstream TFs in these five subnetworks (color-coded and arranged by subnetwork).

Transition from 2D to 3D development is encoded by the DEK1-controlled subnetworks

The subnetworks were functionally characterized via network enrichment analysis (Fig.SF3a) using the developmental stages from the *P. patens* Gene Atlas data (Perroud et al. 2018), PO and GO enrichment analysis (Figs. SF3b-i and Table ST3) as well as manual assessment of experimentally characterized *P. patens* genes (Table ST4). These analyses suggest that subnetworks V (chloronema), II (caulonema, rhizoids, side branch initiation and bud formation) and X (vegetative gametophore shoot and leaf cells) encode the cell types, tissues and developmental transitions most relevant to decipher the DEK1 phenotypes and the 2D to 3D transition (Figs. 2b-d). Subnetwork IX encodes housekeeping gene functions including primary gene regulation, transcription, translation, constitutive epigenetic regulation as well as light-independent mitochondrial and cytosolic metabolic pathways (Figs.2 b,e). Subnetwork VIII harbours the light-dependent and -responsive pathways - in particular photosynthesis, plastid-morphogenesis/ regulation and generally plastid-localized pathways (Figs.2 b,e).

Network structure suggests DEK1-gated sequential transition between cell fates

The majority of regulatory interactions are found within subnetworks (Fig. SF2a). However, as evident from the enrichment of inter-subnetwork connections (Fig. SF2a), the putative indirect DEK1 targets are predicted to be also controlled by regulators from other subnetworks. In order to determine whether the respective TFs act as positive (activators) or negative (repressors) regulators of potential DEK1-controlled gene functions, we studied the directionality of the inter-subnetwork connections based on the sign of the expression profiles' correlation coefficients (black [+] vs. red [-] colored edges in Fig. 2b). Subsequently, we compared the relative proportions of intra- and inter-connections among the enriched subnetworks split according to positive and negative interactions (Figs. 2b,f and SF4).

Strikingly, we found more than expected negative links between V ⊣ II and X ⊣ V (i.e. TFs from V repressing targets in II and X TFs as repressors of V targets) and more positive, activating regulatory interactions between II → X and X → II (i.e. TFs from II activate genes in X and vice versa; Fig. 2f). In our interpretation, this chained pattern potentially reflects the developmental transition between different cell fate identities including primary filament cells differentiating to side branches and gametophore buds. Furthermore, we also observe a biased distribution of *activator* and *repressor* targets among the subnetworks (Fig. 2a). While subnetwork IX is equally enriched for both patterns, V harbours more *repressor targets* and II, VIII and X harbour more *activator targets*. It therefore seems that the enriched subnetworks respond in a specific fashion to the mutation of the plant calpain DEK1.

Taken together, the preferential developmental timing and the biased directionality chain suggest the presence of an inherent directionality of DEK1 action on the regulatory circuitry of these subnetworks. These findings may hint towards a mechanism in which DEK1 affects distinct cellular identities as displayed in the DEK1 mutants.

DEK1 is part of the APB-controlled subnetwork II guarding the 2D-to-3D transition

The directed edges of the GRN graph can be utilized to reconstruct a regulatory hierarchy by ranking the regulators according to network centrality measures like the fraction of a subnetwork that is directly or indirectly downstream and reachable from a given regulator. Applying this *local reaching centrality*

criterion, our analysis identifies the AP2/ERF ANT subfamily transcription factor APB4 as the master regulator at the top of the regulatory hierarchy in subnetwork II (rank 1; reaching >99% of the subnetwork). The eponymous flowering plant members of the ANT subfamily AINTEGUMENTA, PLETHORA and BABY BOOM (APB) are involved in various developmental processes including the formation of the stem cell niche in the Arabidopsis shoot apical meristem (Hata and Kyozuka, 2021). Consistent with the proposed role as master regulators of gametophore apical stem cell formation, timed tissue and cell-type specific expression patterns and the additive, but distinct phenotypic severity of single, double, triple and quadruple knockout mutants of the four moss APBs (Aoyama et al., 2012), the outparalogous gene copies APB2 (rank 35) and APB3 (rank 41) are localized downstream of APB4 in the regulatory hierarchy of subnetwork II. The inparalogous APB1 is localized in subnetwork VII, but is also an indirect target of APB4 (Fig. SF5a). DEK1 is predicted to be localized downstream of APB2 and APB1 in subnetwork II (Fig. SF5b).

The upstream regulatory context suggests that DEK1 is positively regulated by subnetwork V TFs, activated early in development and subsequently negatively controlled by an auxin/ent-kaurene responsive cascade encoded by subnetwork II as well as a hierarchical cascade of SBP TFs in subnetwork X which already has been shown to be involved in bud formation (Cho et al., 2012). In light of the biased directionality chain identified in the DEK1-controlled inter-subnetwork connections (Fig. 2f), this might represent a negative feedback loop buffering the 2D-to-3D transition at the transcriptional level.

Deregulation of GRNs is consistent with DEK1 role as a post-translational regulator

Employing the network structure to trace the upstream regulatory contexts of each target gene in the five DEK1-controlled subnetworks, we further evaluated the validity of the *dual role scenario*. Mammalian calpains direct proteins towards the Arg/N-End Rule Degradatory (NERD) pathway (Piatkov et al., 2014). Thus, the potential direct targets of DEK1 should bear N-terminal amino acid residues marking them for ubiquitylation and subsequent degradation by the proteasome (Fig. 3a). The existence and activity of the NERD pathway has recently been demonstrated in *P. patens* and mutants of a key component are also arrested at the 2D-to-3D transition (Hoernstein et al., 2016; Schuessele et al., 2016). Assuming that DEK1 is acting as a post-translational regulator controlling the half life of transcriptional regulators via the NERD pathway, the majority of deregulated genes in the mutants are expected to be downstream of TFs that are either also deregulated or direct targets of DEK1 calpain cleavage.

To test this, we predicted calpain cleavage sites using GPS-CCD (Liu et al., 2011) and subsequently classified the respective proteins based on overall abundance of putative DEK1 cleavages and prevalence of NERD signatures in the resulting, novel N-termini (Figs. SF6a-f). Strikingly, the three DEK1-controlled subnetworks encoding the 2D-to-3D transition (V→ II→ X) are among the five subnetworks that are enriched for such NERD-like calpain cleavage patterns (Fig. 3a). These three subnetworks also display the highest levels of overall gene deregulation among the five DEK1-controlled subnetworks (X<II<V<IX<VIII; Fig. SF6g). Targets of deregulated TFs are more likely to be deregulated than genes downstream of non-deregulated TFs. While all five subnetworks

display significant, positive correlation of deregulation levels between target genes and their direct upstream TFs (Kendall's rank and Pearson correlation tests; $p<2e-16$), the individual trends for the subnetworks mirror that of the overall gene deregulation levels and confirm the notion that subnetworks X, II and V are most affected by mutation of DEK1 (Fig. 3b). Targets of potentially DEK1/NERD-controlled TFs are consistently more deregulated. As the three subnetworks are also enriched for NERD-like calpain cleavages, we investigated the dependency of these target gene deregulation patterns on putative DEK1 cleavages in their upstream regulons. Indeed, the deregulation levels of the indirect DEK1 target genes in subnetworks II, V and X are positively correlated with the percentage of putative, direct DEK1-targets among their upstream TF cascades (Fig. 3c). The upstream regulons of deregulated genes are significantly enriched for TFs that are indirect and direct targets of DEK1 (87%; Pearson residuals >>4; χ^2 test $p<2e-16$ Fig. 3d). The regulatory cascades demonstrate consistent deregulation patterns. The direct upstream regulons (first order: TF→target) are mostly deregulated themselves. I.e. they are either indirect DEK1 targets because their upstream TF is controlled by DEK1 (Fig. 3d left lower box) or are both direct and indirect DEK1 targets. These TFs are directly cleaved by DEK1 and deregulated in the mutants because an upstream, higher order TF is a direct DEK1 target (Fig. 3d lower right box). Consistently, second (TF→TF→target) and third (TF→TF→TF→target) order regulons of deregulated genes are enriched for predicted direct cleavage by the calpain (Fig. SF6h).

Filtering of the DEK1-controlled regulons to first order interactions results in 531 TFs that are predicted to be direct calpain cleavage targets (Figs. 3e and SF7a). These TFs are predicted to directly regulate the expression of 3,679 significantly deregulated target genes, i.e. genes that are under indirect control of DEK1 (Table ST6). 85 TFs fall in both categories, i.e. are potential direct and indirect DEK1 targets. These predicted first order DEK1 targets form a highly interconnected network, comprising a total of 10,120 network edges (Fig. SF7b). The majority of these genes (74%) are encoded by the five major DEK1-controlled subnetworks (Figs. 3e and SF7a). 73% of the inherent 4,082 inter-subnetwork connections target one of the five subnetworks (Fig. SF7c). More than half of these target genes in the three subnetworks are involved in the 2D-to-3D transition (V, II and X). This is also confirmed by results of an ontology analysis that suggests clear functional delineation of biological processes implemented by the DEK1-controlled repressive and activating intra- and inter-subnetwork regulatory interactions (Figs. 3f-g and SF8a-e).

Taken together, by tracing the upstream regulatory cascades of deregulated target genes, we observed consistent TF-target deregulation patterns and found an enrichment of predicted calpain cleavages at the starting points of such deregulated cascades. These findings are in line with the *dual role scenario*, i.e. support the role of DEK1 as a post-translational regulator controlling the half lives of many genes via the regulatory layers especially in subnetworks II, V and X and thereby gating the sequential transition between the encoded cell fates. Further functional characterization of the predicted first order DEK1 target genes should therefore shed light on the molecular factors underlying the pleiotropic DEK1 phenotype and role in plant development.

Candidate targets suggest deep conservation of DEK1 control over plant development

Target genes from subnetworks X, II and V positioned downstream of DEK1-controlled activators are enriched for biological processes, cellular components and plant anatomical entities (color text; Figs. 3e, f, g and SF8a) which can be directly linked to the observed DEK1 mutant phenotypes and tissue and cell-type specific expression profiles of DEK1 in flowering plants and the moss (Tian et al. 2007; Perroud et al., 2014; Demko et al., 2014; Amanda et al., 2016; Johansen et al., 2016; Perroud et al., 2020).

The predicted DEK1-controlled genes regulate or comprise components determining cell polarity, cell axis, cell number, division, division plane and cell fate. These are involved in biological processes including *regulation of asymmetric cell division* (e.g. by STRUBBELIG orthologs; Chevalier et al., 2005), *callose deposition in cell walls* (Panteris et al., 2021) and defined cellular components including the *phragmoplast* (e.g. orthologs of AUG6, Lee et al., 2017 and TANGLED1, Martinez et al., 2020) and the *cell plate* (e.g. STRUBBELIG orthologs or CLAVATA1/*Pp*CLV1b, Whitewoods et al., 2018).

Besides these specific processes and compartments, the predominant pattern is consistent with the role of DEK1 as regulator governing developmental processes. DEK1 mutants are disturbed in processes involving general cell fate determination or transition and stem cell, meristem or primordium identity and initiation (e.g. shoot, flower, root and axillary bud meristems; development of endosperm, ovule and embryonic meristems; Fig. 3f). Also, enrichment of anatomical entities among the DEK1 target genes from subnetworks X, II and V include components expected to be affected in DEK1 mutants (Fig. 3g). These include cell types such as the *leaf lamina* (Hibara et al., 2009), *epidermal initial cell* (Galletti et al., 2015) or the *meristem L1 layer* (Olsen et al., 2015). The latter provides two striking examples where orthologs of the predicted, indirect DEK1 targets have been confirmed to be also deregulated in flowering plant DEK1 mutants (HD-Zip-IV TF MERISTEM LAYER 1 Galetti et al., 2015; CLV3 Liang et al., 2015).

Experimental evidence from *P. patens* contained in Plant Ontology annotations, points to an enrichment of the cell types *protonema sub-apical initial cell* and *gametophore bud*. Both are the two major, sequentially occuring cell types related to the 2D-to-3D transition (i.e. gametophore bud formation). The former is the site for the positioning and initiation of a new apical stem cell inside a growing, primary filament that can either develop into a secondary protonemal side branch or give rise to a three-faced gametophore bud initial, which is the apical stem cell developing into the 3D gametophore. Both cell types have been extensively studied and have been genetically linked to central, conserved developmental regulators acting in both flowering plants and the moss, like e.g. the APB and CLAVATA genes (Aoyama et al., 2012; Whitewoods et al., 2018). This supports a deep evolutionary conservation of the underlying developmental processes that seem to be controlled by DEK1.

Tracing the deregulated molecular actors of the complex, pleiotropic DEK1 phenotype in the GRN

To understand the role of the predicted DEK1 targets in these conserved developmental processes and their role in the pleiotropic DEK1 phenotype, we established a protocol to predict genes underlying

specific phenotypic characteristics of the DEK1 mutant strains. The developed Factorial Differential Gene Expression Network Enrichment Analysis (FDGENEA) method utilizes phenotypic traits encoded as binary factors (Fig. SF9a) for differential gene expression analysis. The resulting differentially expressed genes displaying significantly altered transcript abundances in association with one of the 17 phenotypic factors (Table ST8), were then traced in the GRN to identify the predominantly affected subnetworks (Fig. SF9b,e).

Again, the observed, significant network associations demonstrate the importance of subnetworks X, II and V to explain the DEK1 phenotype (FDR<0.01; Fig. SF9b). The resulting FDGENEA sets overlap, but also display substantial portions of genes that are specifically deregulated in response to a single trait (Fig. SF9f). The assessed phenotypic traits clearly separate into two classes that are enriched for either DEK1-controlled *activator* or *repressor targets* (Fig. SF9g; comprising 2,048 indirect DEK1 targets).

Ectopic gametophore initiation in the mutants can be traced to the deregulation of DEK1-controlled genes with bud cell-specific expression profiles in subnetworks II and X

The earliest step of the 2D-to-3D transition that appears to be disrupted in the DEK1 mutants, is the initiation of gametophore apical stem cells along the protonema filaments. Phenotypically, this is particularly pronounced in the number of buds per filament and the percentage of filaments with buds (Fig. 1c). While the *oex1* line forms fewer, the *Δdek1* and *Δloop* lines develop significantly more buds per filament than the wild type (ANOVA with post-hoc LSD $p<0.05$). This latter *overbudding* phenotype (Fig. 4a) is consistent with a disrupted control of gametophore initiation, leading to ectopic formation of 3D apical stem cells. It shows the largest unique set of deregulated genes in the FDGENEA of this group of traits (Figs. SF9h; Table ST8) and is enriched for genes from subnetworks II, V, IX, X and XI (Figs. 4a, b and SF9c, e).

The affected parts of the GRN (Figs. 4a and SF9c, d) can be partitioned into three groups of nodes. Two groups correspond to genes that are either positively associated with a high number of buds (*overbudding-up*; i.e. up-regulated in *Δdek1* and *Δloop*; right group in Fig. 4a and SF9c, d) or those that display a negative association (*overbudding-down*; i.e. down-regulated in *Δdek1* and *Δloop*, but up-regulated in WT, *oex1* and *Δlg3*; left group in Fig. 4a and SF9c, d). The third group is composed of their direct upstream regulators without significant change in expression with respect to this phenotype (top group in Fig. 4a and SF9c, d). The clustering reveals also a trend in the type of connections between the first two groups that also harbor negative regulatory interactions (orange edge color; Fig. 4a and SF9c, d). Overall, while subnetwork V dominates the *overbudding-down* group, the *overbudding-up* assemblage is more diverse and consists of subnetworks X, IX and XI (Fig. 4b and SF9c). Subnetwork II is prominent in both groups. Negative inter-subnetwork links predominantly involve nodes between subnetwork V and either II or X. Subnetworks II and X as well as IX and XI seem to act in conjunction, i.e. share many positive edges (Fig. SF9c). These patterns are consistent with the global network structure discussed above (Fig. 2f) and the sequential transition between the encoded cell fates (Fig. 4f) from primary filament cells (V) redifferentiating to pluripotent side branch

initials, that give rise to either secondary chloronemal (V) or caulonemal filaments (II) or gametophore buds (X).

The set of genes up-regulated in filaments displaying the *overbudding* phenotype is dominated by indirect and direct DEK1 targets from subnetworks II, IX and X (Fig. 4b). Down-regulated genes are either not targeted by DEK1 or encoded by subnetwork V or IX. There is a significantly larger proportion of DEK1-controlled regulatory interactions for *overbudding* associated genes in subnetworks II and X (Table ST9). Subnetwork V displays more non-DEK1 controlled interactions, most being negatively associated with *overbudding*. While these regulatory interactions likely represent the side-branch initials redifferentiation into secondary chloronema (Fig. 4f; lower row), the *overbudding* up-regulated, predominantly DEK1-controlled interactions in subnetworks II and X likely encode the cell fate transitions required to establish the gametophore apical meristem (buds).

Consistently, the set with positive association to *overbudding* (*up* in Fig 4b) is enriched for DEK1-controlled *activator targets* from subnetwork II and X which have been previously identified to be specific to gametophore bud cells, while down-regulated genes from V are predominant in the protonemal tip cell transcriptome (Frank and Scanlon 2015). *Overbudding*-associated genes from subnetworks IX and XI are more likely to be found in both transcriptomes, hinting at their more ubiquitous expression profiles or housekeeping function. The bud-specific portion of *overbudding-up* DEK1 targets reveals 248 genes (Table ST10). The majority (73%) is encoded by subnetworks II (62; 25%) and X (118; 48%). Thus, the DEK1-controlled, *overbudding* up-regulated *activator targets* from subnetworks II and X represent prime suspects to harbour the developmental regulons acting in the cell fate transitions involved in gametophore apical stem cell initiation which is so pivotal to the 2D-to-3D transition.

Predicted *overbudding* up-regulated DEK1 targets comprise an interconnected regulon with many known molecular actors of meristematic cell fate specification in moss and flowering plants

Network analysis reveals that around 51% of the 901 *overbudding-up* DEK1 *activator targets* form an interconnected regulon (Fig. SF9i). Given the post-translational role of DEK1, a direct cleavage target will not be deregulated in the mutant context unless an upstream regulator is also a direct cleavage target. Thus, a regulon solely inferred based on the *overbudding-up* genes will be an underprediction. Indeed, when we extend the regulatory context of these genes to include the up to five highest ranking DEK1-controlled upstream TFs, 100% of the *overbudding-up* genes are interconnected (Fig. SF9j).

The *overbudding-up* components of the regulon reveals that the majority is controlled by two regulatory circuits from subnetworks II and X (Fig. SF9i). The first circuit is dominated by TFs from the AP2 superfamily in subnetwork II and comprises several well-characterized key players in meristematic cell fate regulation of flowering plants and *P. patens* (DRN, DRNL and PUCHI Chandler and Werr 2017, STEMIN3 Ishikawa et al. 2019 , APB-3 Aoyama et al., 2012). The second circuit is dominated by subnetwork X encoded, gibberellin-responsive MYB TFs that have been shown to orchestrate reproductive organ development as well as the production of extracellular hydrophobic barriers like the cuticle and sporopollenin of flowering plants and the moss (GAMYB2 Aya et al., 2011;

MYB80 Xu et al., 2014; MIXTA Oshima et al., 2013). While the two circuits are mostly insulated, some of the target genes overlap (17% of *overbudding-up* only- and 35% of the extended regulon; Figs SF9l, m). At the regulatory level, this insulation might be unidirectional in that one of the subnetwork X MIXTA orthologs is predicted to positively regulate a DRN and a DRNL ortholog in subnetwork II. This might represent a positive feedback mechanism.

Target genes of both circuits are involved in reorientation of the division plane, modulation of the cell wall, the cytoskeleton and the phragmoplast (e.g. Fig. 4a). Moreover, they encompass a notable accumulation of components required for generation, transduction and perception of local queues like mechanical stress (MSCL16 Wilson et al., 2013) and longer distance, gradient-forming, developmental signals like plant peptide hormones (CLV1b, CLE9 Whitewoods et al., 2018) or the phytohormones auxin, gibberellin, strigolactone and cytokinin. The latter is especially noteworthy. While the other three phytohormone pathways are represented by one or two components involving either transport (LAX2 Swarup and Bhosale 2019), biosynthesis (GA2ox4 Miyazaki et al., 2018; CCD8 Proust et al., 2011) or activation (GA20ox6 Miyazaki et al., 2018), in the case of cytokinin, all major aspects are covered. The regulon comprises several genes encoding biosynthesis (IPT3 Lindner et al., 2014), activation (LOG Kuroha et al., 2009), degradation (CKX Schwartzenberg et al., 2007), transport (ENT, ABCG Borghi et al., 2015) perception (CHK1, CHK2 Schwartzenberg et al., 2016) and transduction (ARR To and Kieber 2008) of cytokinins. In addition, the MYB circuit of the regulon also is predicted to induce cytokinin-responsive genes like NO GAMETOPHORES 2 (NOG2 Moody et al., 2021), whose loss-of-function mutant similar to DEK1 also displays an *overbudding* phenotype. Consistently, the exogenous application of cytokinin (Schwartzenberg et al., 2007) and cytokinin-overproducing mutants (Schulz et al., 2000) also result in an *overbudding* phenotype. These findings clearly demonstrate the conservation of hormonal control in stem cell initiation and cell fate specification in land plants (Lee et al., 2019).

As mentioned above, the regulon also comprises essential components of the CLAVATA (CLV) peptide and receptor-like kinase pathway that has been shown to control cell fates and division planes of land plant apical stem cells (Fletcher et al., 1999; Whitewoods et al., 2018; Hirakawa et al., 2019) via CLV3/EMBRYO SURROUNDING REGION-Related (CLE Yamaguchi et al., 2016) peptide hormones which are perceived and transmitted to downstream signalling cascades via CLV1-type receptor-like kinases (Hazak and Hardtke 2016). Several studies in both Arabidopsis (Johnson et al., 2008) and Physcomitrella (Whitewoods et al., 2018; Moody et al., 2018; Moody et al., 2021) already have identified parallels in mutant phenotypes and expression patterns and have proposed models locating the CLV signalling pathway somewhere downstream of DEK1 and the moss APBs. The predicted *overbudding-up* regulon identified here, now provides us with a robust explanation for these connections. Our predictions indicate that CLV1b and CLE9 are an integral part of the regulon that is downstream of both of the above DEK1-controlled circuits (Figs. SF9i,k) - in particular downstream of APB-3 (Fig 4c). APB-3 is predicted to coordinate its control over these genes with a calmodulin-binding WRKY group II transcription factor (WRK7 Park et al., 2005), that could act to integrate a possible Ca^{2+} signal emerging in response to the swelling of the gametophore initial cell (Tang et al., 2020). Furthermore, our calpain cleavage predictions indicate cleavage sites that would

allow the maturation of CLE peptides from their respective preproteins encoded by the *P. patens* genome (Whitewoods et al., 2018, Supplementary File `PpCLEs.ccd.all`). This could represent another potential feedback layer of the regulon in that CLEs are both positively (maturation/activation) and negatively (indirect *activator targets*) controlled by DEK1. The second order regulatory context of CLV1b (Figs 4c and SF9k) suggests that all positional and developmental queues discussed above are co-regulated in one DEK1-controlled *CLAVATA regulon*. Consistent with the findings from two recent studies (Nemec Venza et al., 2021; Cammarata et al., 2021), our data suggests that this DEK1-controlled, cytokinin-mediated pathway governs stem-cell homeostasis separately from the cytokinin-independent pathway involving the RECEPTOR-LIKE PROTEIN KINASE2 (RPK2; subnetwork VIII).

The *overbudding-down* part of the GRN is controlled predominantly by MADS box TFs, contains several correctly predicted, negative regulators of bud and gametophore formation (e.g. DEK1 Demko et al., 2014; PHK2 Ryo et al., 2018) and is enriched for cytoskeletal components involved with polarized tip growth of protonemal filaments (e.g. FOR1D Vidali et al., 2009; SPR2 Leong et al., 2018). Plant Rho GTPases (ROP) are key regulators of cellular polarization and are involved in several symmetry breaking mechanisms (Eklund et al. 2010; Muñoz-Nortes et al. 2014). Activated ROP binds effector proteins e.g. to initiate remodelling of the cell wall (Cheng et al. 2020) or the cytoskeleton (Muñoz-Nortes et al. 2014). Sometimes they act as transducers for receptor-like kinases (Jose et al., 2020). The *P. patens* ROP4 is localized at the tip of a growing protonema filament and relocalizes prior to protonemal branching to the future site of side branch formation (Cheng et al. 2020). ROP4 is predicted to be an *overbudding-down* DEK1 *repressor target*. Rho GTPase-dependent signalling by ROPs is tightly controlled at the protein level (Eklund et al. 2010). ROPs are activated by RhoGEFs, while RhoGDIs and RhoGAPs provide independent means of ROP inactivation. Our analysis detected a representative of both ROP-regulator types as *overbudding*-associated, indirect, DEK1-targets with opposing regulatory patterns (DEK1 *activator target*, *overbudding-up,* part of the *CLAVATA regulon*: ROP-GEF, Pp3c10_9910; DEK1 *repressor targets*, *overbudding-down*: RhoGAP, Pp3c3_5940 and RhoGDI, Pp3c10_19650). This observation is consistent with their proposed antagonistic role in controlling ROP signalling. It provides a compelling example of how DEK1 might post-translationally control asymmetric and other types of formative cell division by remodelling of cell walls and the cytoskeleton.

Discussion

The plant calpain DEK1 acts as a post-translational regulator of protein stability and gene expression

In our study we contrasted two scenarios concerning the functional role of the calpain DEK1 in the developmental regulation of plant cell fate transitions. In the first scenario DEK1 solely acts as a modulatory protease that alters the activity of a limited number of specific proteins in and around the cell wall, cytoskeleton and cell division apparatus thereby primarily acting on the physical layers of cell fate transitions. In the second scenario proteolytic cleavage by DEK1 can have both modulatory and destabilizing consequences for a larger set of target proteins in both the physical and the regulatory layers of cell fate transitions. The destabilizing DEK1 cleavages contain signatures targeting the fragments to the NERD pathway and ultimately towards degradation by the proteasome. As this post-translational regulation also comprises TFs and other gene regulators, DEK1 indirectly controls the expression of many target genes.

By tracing the deregulation profiles of DEK1 null and over-expressor mutans in the gene regulatory networks of the moss *P. patens*, we identified at least 3,679 consistently deregulated genes whose expression is controlled by 531 TFs containing such destabilizing calpain cleavage sites. These TFs are thus direct targets of the plant calpain that in turn acts as an indirect regulator of downstream target genes. The observed deregulation is not limited to the target genes but can be traced through the regulatory hierarchy revealing consistent predicted cleavage sites and mutant deregulation levels of TFs including the master regulators of the respective subnetworks. Individual master regulators but also more downstream TFs and many of the target effector genes have already been experimentally tied to specific DEK1 phenotypes in *P. patens* and flowering plants. Integrating over all observations, we conclude a dual role of DEK1 as a modulatory and destabilizing protease acting on the physical and regulatory layers of cell fate transitions and thereby indirectly controlling many gene functions.

The role in post-translational gene regulation and predicted list of DEK1 targets provides a consistent explanation for the calpain's essentiality, pleiotropy and broad effects observed in the moss and also many of the reported phenotypes and genetic interactions in other plants and eukaryotes. Considering that these predictions do not take secondary and tertiary structure, and thus site accessibility, into consideration, the raw number of predicted calpain cleavage sites seem like an overestimate. In light of the multiple layers of regulation and presumed preferential cleavage within unstructured, inter-domain regions reported for metazoan calpains (Ono and Sorimachi, 2012), the true number of *in vivo* cleavage sites must be lower also *in planta*.

We based our predictions on the mutant expression profiles in combination with the inferred gene regulatory networks. The stringently filtered, NERD-classified, predicted calpain cleavage sites were utilized for confirmation. Nevertheless, the detected broadness of those filtered cleavage sites, especially in transcription factors and other gene regulators, is consistent with the observed broad transcriptional, functional and phenotypic responses in *P. patens*.

DEK1 controls developmental cell fate transitions implemented by deeply conserved land plant regulons

Individual examples like ROP signalling or the above described *CLAVATA regulon* may help to bridge the gap between the well-established image of DEK1 as a developmental regulator that is affecting cell fates and division plane reorientation, and the role as a post-translational regulator proposed here. Our analyses suggest the existence of deeply conserved, orthologous, hormone-guided regulons governing land plant meristems and stem cells that are post-translationally controlled by DEK1 acting as a fine-tunable reset switch implementing or guarding the transition between different cellular identities. The documented, high level of conservation again highlights the utility of the model plant *P. patens* to elucidate embryophyte development and stem cell regulation. In case of the *overbudding* phenotype i.e. the initiation of gametophore apical stem cells, DEK1 is a negative regulator of cell fate transitions. It thus acts as a repressor of the 2D-to-3D transition. Combined with the gene regulatory networks and functional predictions, the DEK1 mutants thus provide a framework to identify and mechanistically characterize the players involved in this crucial developmental transition.

Model of a fine-tunable, developmental switch gatekeeping cell fate transitions

In our model (Fig. 4d-f), the level of active calpain is tightly controlled and fine-tunable on multiple levels. DEK1 integrates multiple developmental signals (e.g. phytohormones, peptides, light, mechanical stress) and acts as a gatekeeper in the transition between distinct cellular fates (Fig. 4f). The transcriptional profiling of the four distinct DEK1 mutants enabled us to monitor three extreme points in the distribution of calpain activity i.e. the number of direct and indirect targets ($N_{targets}$; *off=Δdek1*, *Δloop*; *few=Δlg3*; *many=oex1*; Figs. 4d,e). In our model for gametophore bud formation, the level of calpain activity is proportional to the probability (P_{bud}; Fig 4e) of a side branch initial developing into a gametophore initial cell (Fig. 4f).

The immobile, inactive, full-length DEK1 protein (*off*; Fig. 4d) resides in the plasma membrane (Tian et al., 2007; Johnson et al., 2008; Perroud et al., 2020) and can potentially be phosphorylated at several sites (Nühse et al., 2004; Nakagami et al., 2010), probably resulting in conformational changes and (de)activation. While animal calpain activity depends on Ca^{2+} binding (Moldoveanu et al., 2002), it is currently unclear to what extent Ca^{2+} activation is required for the DEK1 calpain's *CysPc-C2L* protease domain (Wang et al., 2003; Tran et al., 2017). The autocatalytic activity of DEK1 (Johnson et al., 2008; Supplementary File `DEK1.jvp`) likely results in a short half-life of the mobile, unconstrained calpain that would target *many* proteins potentially acting as a reset switch of a cell's protein complement (*many*; Fig. 4d).

However not all potential cleavages bear destabilizing N-terminal residues targeting a protein towards degradation by the proteasome via the NERD pathway (Fig. 3a). Depending on the amino acid signature of the new N-terminus, the resulting polypeptide is either NERD-directed or stable and may represent the activated or mature form of the protein or peptide (e.g. CLEs). This seems also true for DEK1 itself. Our data suggest the existence of at least three stable calpain variants that potentially arise by auto-catalytic cleavage in the Linker_LG3 domain (Supplementary File `DEK1.jvp`). These are similar to the sizes of experimentally confirmed forms in Arabidopsis (Johnson et al., 2008). The

varying N-terminal regions resulting from such cleavages might either lead to different half-lifes or enable binding of different cofactors potentially modifying specificity or the calpain's target range (*few*; Fig. 4d).

We also found components of the NERD pathway (e.g. orthologs to crucial N-recognins PRT1 and PRT6; Fig. 3a; Holdsworth et al., 2020) among the indirect DEK1 targets. These potentially represent yet another regulatory layer, allowing to switch off degradation or fine-tune protein stability and balance post-cleavage protein fates towards the modulator activity i.e. activation or maturation (Fig. 4d).

Dual role as a modulatory and destabilizing protease

Mechanistically, calpain research so far has largely focused on the role as a non-processive, modulatory protease (Storr et al., 2011; Sorimachi and Ono, 2012; Ono and Sorimachi, 2012). Whereas its destabilizing characteristics, observable e.g. in the coactivation with the ubiquitin-proteasome system (Freitas et al., 2016) and the generation of short-lived substrates for the NERD pathway (Piatkov et al., 2014), have not yet received much attention. At the same time, many of the experimentally characterized calpain targets (Shinkai-Ouchi et al., 2016), especially those with confirmed NERD degrons (Piatkov et al., 2014), are involved in transcriptional or other forms of gene regulation. The functional implications of this have so far been under-investigated.

In plants, it has been difficult to align the observed directionality (activation vs. inactivation of biological functions), impact, pleiotropy and severity of DEK1 phenotypes with the role as a modulator protease. This changes by extending our view to also include the role as upstream component of the ubiquitin-proteasome system (Varshavsky, 2012) that directs proteins via the route of the NERD pathway. Destabilizing calpain cleavages in TFs effectively can inhibit the expression of all downstream target genes and thus indirectly regulate gene expression. The substantial changes in gene expression observed in the DEK1 mutant lines are most parsimoniously explained by the model that proposes DEK1 to act as a post-translational regulator by indirectly controlling the half-life of transcriptional regulators. Nevertheless, DEK1 like other calpains remains a non-processive and modulatory protease. Our predictions do hint at the importance of DEK1 in protein maturation and activation (e.g. DEK1 and CLEs). Thus, we propose a duality of outcomes for proteolysis by calpains (Fig. 4d). Our data in *P. patens* indicate that in most cases the final outcome of such cleavages will result in degradation by the proteasome. Given that calpains frequently are characterized as deleterious, aggravating factors of human pathological conditions (Storr et al., 2011; Sorimachi and Ono, 2012) and the ratio of confirmed NERD-targets among calpain substrates (Piatkov et al., 2014), this might also be a viable and resilient hypothesis for mammalian calpains.

Calpains are involved in a vast spectrum of biological processes and are controlled at multiple levels (Storr et al., 2011; Sorimachi and Ono, 2012; Ono and Sorimachi, 2012). On the evolutionary timescale, the emergence of a novel calpain cleavage site can be considered a random event with either a positive outcome (i.e. a functional neo-protein) or more frequently a negative outcome (i.e. a detrimental fragment). Without the tight regulatory constraints, the fuzzy target specificity and the ubiquitous expression of calpains likely would result in a myriad of fragments and neo-proteins. This

necessitated mechanisms that favour functional neo-proteins while simultaneously avoiding or controlling deleterious fragments. The proposed dual role as a modulatory and destabilizing protease acting in the modulation of a fraction of protein functions on the one side, while directing the majority of detrimental cleavage fragments towards the NERD pathway on the other, provides the most parsimonious explanation for what we observe in extant organisms. The gene regulatory consequences of the resulting NERD-control over calpain-targeted TFs subsequently allowed to establish this as a regulatory mechanism in form of a post-translational gatekeeper of cell fates. The fact that DEK1 is found as a single copy gene in most land plants argues for a crucial and dosage-sensitive role of the plant calpain (Zhao et al., 2012; Demko et al., 2014; Harrison J., 2015).

New approach to genotype-phenotype mapping and the mechanistic exploration of calpains

The systematic and large-scale analysis or discovery of calpain targets so far has been hindered by the limited target specificity, involvement in a broad spectrum of biological processes and complexity of regulatory mechanisms. Piatkov et al. (2014) even go as far as to state: "Natural calpain substrates were identified thus far largely by serendipity, as distinguished from proteome-scale surveys". Considering the confirmed calpain targeted human gene regulators and the various reports of gene deregulation in metazoan calpain mutants and human pathologies (Miyazaki et al., 2016; Oliver et al., 2018; Tian et al., 2020), a gene regulatory role might also be true for metazoan calpains. The approach chosen here, i.e. tracing calpain mutant or pathological deregulation profiles in GRNs to identify indirect and direct targets, might thus help to elucidate this yet under-explored aspect of calpain biology in general. The developed FDGENEA method can also prove to be invaluable to other sorts of genotype-phenotype mappings. The outcome of the approach is particularly fruitful for calpain research. The obtained genome-wide and unbiased target candidate gene lists serve as valuable starting points to gain further momentum in the mechanistic exploration of this enigmatic and important proteolytic system with important regulatory and developmental implications in all eukaryotes.

Acknowledgments

The research reported herein was made possible by FRIMEDBIO grant 240343 from the Norwegian Research Council to OAO. The sequencing service was provided by the Norwegian Sequencing Centre (www.sequencing.uio.no), a national technology platform hosted by the University of Oslo and supported by the *Functional Genomics* and *Infrastructure* programs of the Research Council of Norway and the Southeastern Regional Health Authorities. VD was supported by the Slovak Research and Development Agency grant APVV-17-0570.

Author Contributions

OAO initiated and designed the *P. patens* mutant study and contributed to writing the manuscript. VD carried out the *P. patens* wet lab experiment including microscopy, observations and interpretations, contributed to the phenotypic factor annotations, performed RNA extraction, genotyped the *oex1* line, prepared Figs. 1b-c and SF9a and contributed to writing the manuscript. TB performed initial

computational analysis of the DEK1 RNA seq data. MM performed QC of the DEK1 RNAseq data and contributed to the initial DEK1 RNA seq analysis. TH contributed to the initial computational analysis of the DEK1 RNAseq data. PFP contributed to the initial DEK1 RNAseq data analysis, created the *oex1* line and contributed to the phenotypic factor annotations. KFXM contributed to writing the manuscript. DL conceived, designed, implemented and carried out all presented data analyses (final DEK1 RNA and global RNA seq analyses, GRN inference and analysis, calpain target predictions, phylogenomics, ontology and other functional annotations, enrichment analyses, FDGENEA...), postulated the DEK1-NERD hypothesis, wrote software, created and curated data sets, prepared the figures and wrote the manuscript.

Declaration of interests

The authors declare no competing interests.

Figure titles and legends

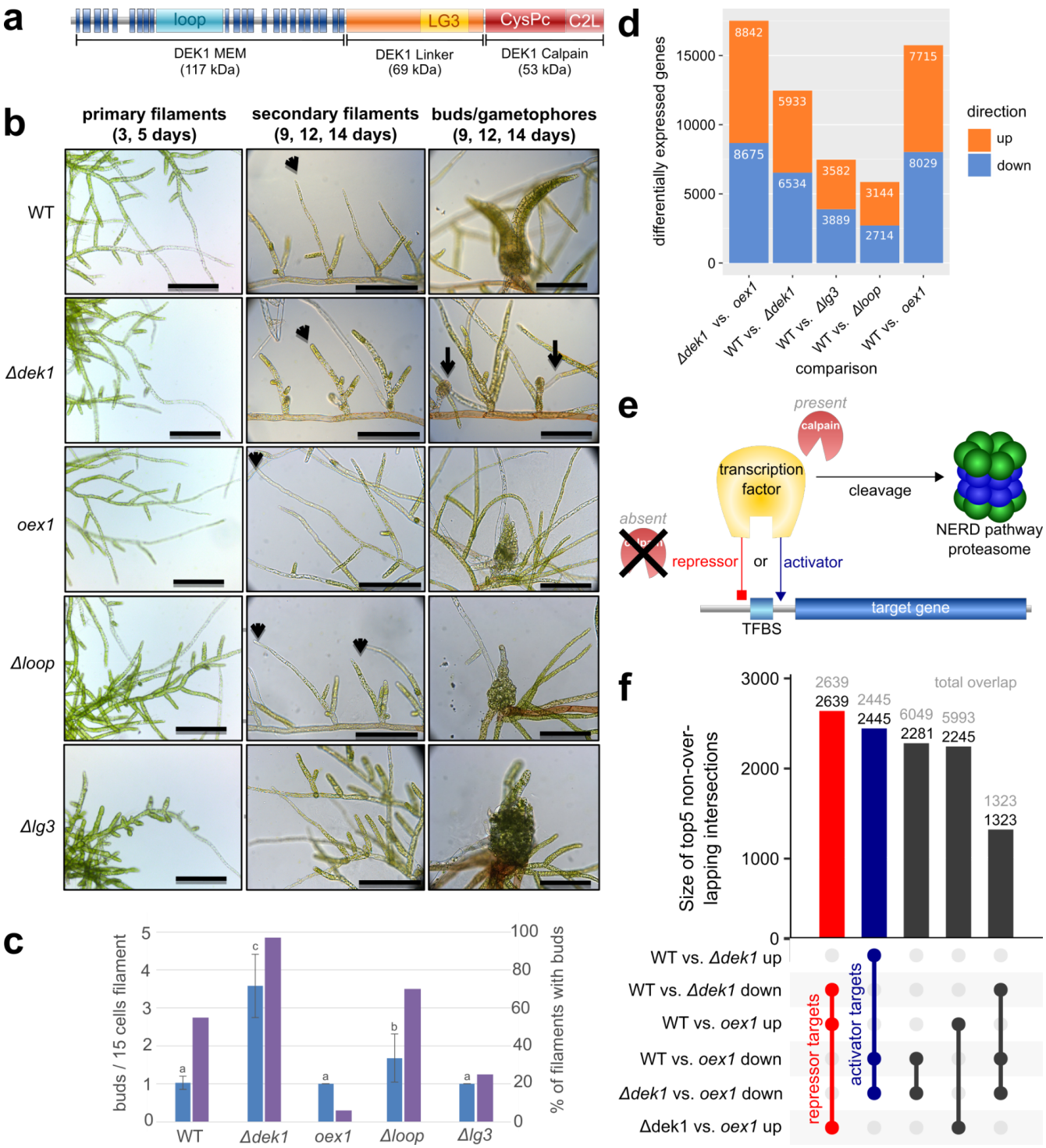

Figure 1. Phenotypes and transcriptome of *DEK1* mutant lines in *P. patens*. a. DEK1 protein domain structure. **b.** Time series analysis of *P. patens* juvenile gametophyte development in wild type (WT), a DEK1-Calpain domain over-expressor (*oex1*), a complete deletion of the DEK1 gene (*Δdek1*; Perroud et al. 2014) as well as two partial deletion lines lacking the loop (*Δloop*; Demko et al., 2014) and the LG3 domain (*Δlg3*; Johansen et al. 2016), respectively. Microscopic images (scale bars:

200µm) depict primary filaments in early stages of protonemata development (left column), secondary filaments (middle column, arrowheads point to apical cells of individual secondary filaments), buds and gametophores (right column, arrows point to arrested buds in *Δdek1*). **c.** Quantitative analysis of gametophore apical meristem (bud) formation in DEK1 mutants. Frequency of meristem initiation expressed as number of buds per 15 cell long filament (blue bars; left x-axis) and percentage of filaments forming buds (purple bars; right x-axis). Statistical significance at 95% confidence is indicated for mean values (a, b, c). Analysis of variance (ANOVA) and least significant difference (LSD) was performed in multiple sample comparisons. **d.** Pairwise, differential time-series gene expression analysis of DEK1 mutants at 3, 5, 9, 12 and 14 days. Stacked bar chart of significantly differentially expressed genes (DEGs) at false discovery rate (FDR) <10%. Fill colors correspond to up (orange) and down-regulated (lightblue) genes. **e.** Model hypothesis for the gene regulatory role of DEK1/calpains. Model depicts two states: When the active calpain is present: TF (transcription factor) is cleaved and targeted to the N-end rule degradatory (NERD) pathway, resulting in lack of gene regulation. In the absence of an active calpain the TF regulates target gene expression either as an activator (blue) or repressor (red). **f.** Size of the top 5 intersections between the sets of DEGs in panel d. Numbers above the bars depict the unique (black) and the total (grey) size of each intersection. The two largest unique intersections correspond to expression profiles consistent with a reciprocal deregulation in *Δdek1* and *oex1*. The largest set (red) comprises 2,639 genes which are down-regulated in *Δdek1* and up-regulated in *oex1*. This profile is consistent with the hypothesis that these genes are targets of DEK1-controlled repressors. The second largest set (blue) comprises 2,445 genes that are up-regulated in *Δdek1* and down-regulated in *oex1*. These genes are likely controlled by DEK1-targeted activators.

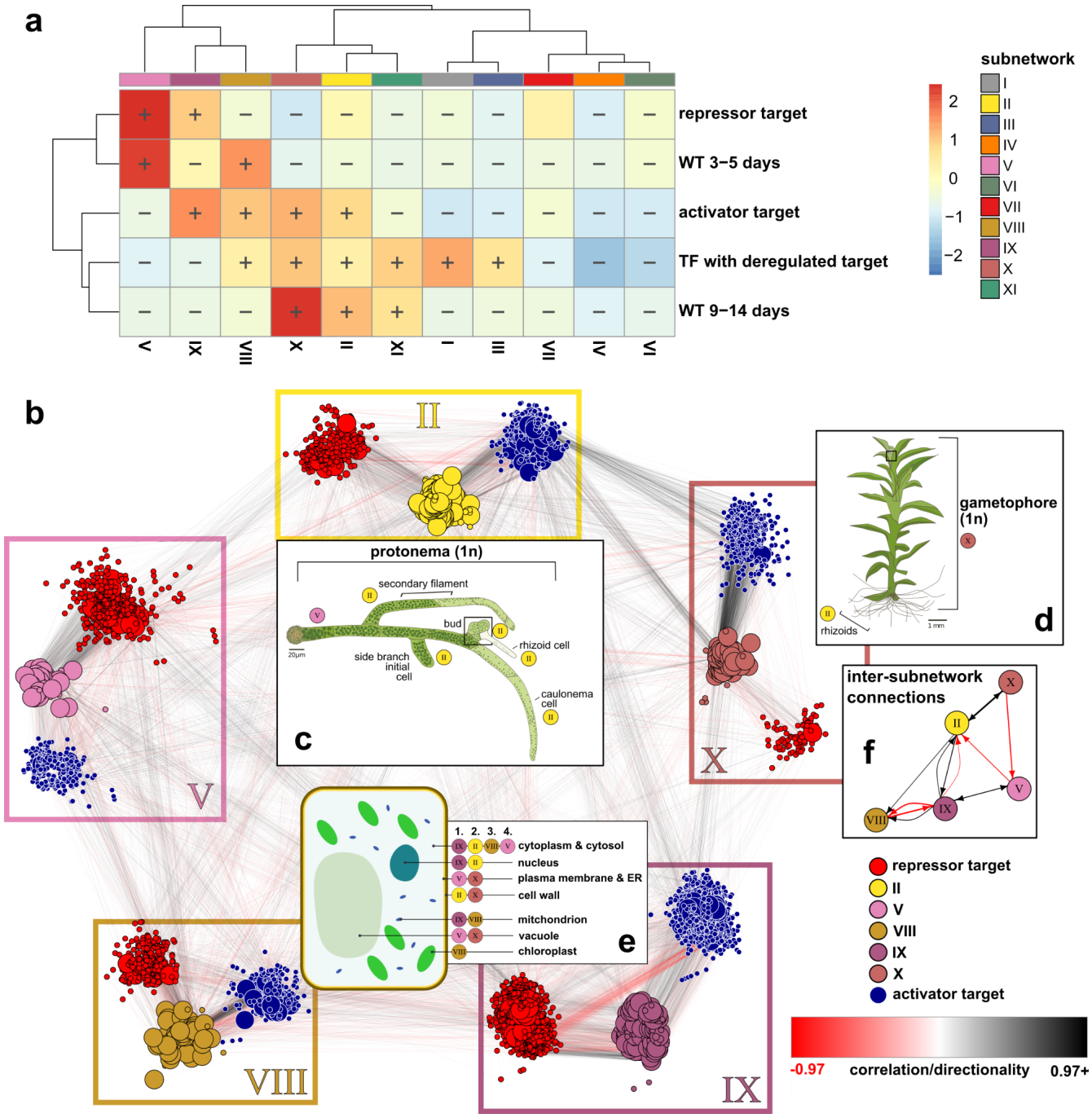

Figure 2. Tracing DEK1-deregulated genes and their upstream regulators in the predicted *P. patens* gene regulatory network (GRN) highlights the subnetworks that are encoding the developmental transitions governed by the calpain. Prediction of regulatory interactions with subsequent community clustering resulted in 11 subnetworks (Fig. SF2a). **a.** Network enrichment analysis highlights specific subnetworks as over-represented among DEK1-deregulated gene sets (activator and repressor targets) and their upstream regulators (TF with deregulated target) as well as the distinct phases of wild type development (WT 3-5 and 9-14 days). Heatmap depicting ratio of observed vs expected sizes of specific candidate gene sets among the identified subnetworks. Significant (FDR<0.01) enrichment (+) or depletion (-) is presented by respective heat map cell

annotations. Ratios were clustered for rows and columns using the ward.D2 method. **b.** Network graph of the five DEK1-deregulated subnetworks: For each enriched subnetwork (II, V, VIII, IX and X), all genes with an activator (blue nodes) or repressor (red nodes) deregulation pattern in the DEK1 mutants (Fig. 1f) are depicted as nodes together with unchanged, direct upstream TFs (using subnetwork color code) as a triangular subgraph in subnetwork-colour-framed boxes. Node sizes are scaled by local-reaching centrality, i.e. the fraction of the total subnetwork that can be reached via regulator→target connections. Edges, representing the predicted regulatory interaction between a TF and its target, are coloured according to putative directionality. According to this color scheme, negative, repressive interactions are red and positive, activative regulatory interactions are black. Inlets **c.** and **d.** depict significantly enriched developmental stages and tissue or cell types. **c.** Drawing of the predicted roles of subnetworks V and II in the different cell fates comprising the haploid protonema stage. **d.** Drawing of the haploid, leafy, juvenile gametophore which, except for the filamentous rhizoids that are encoded by subnetwork II, is predominantly implemented by subnetwork X. **e.** Drawing of a plant cell depicting the significantly enriched intracellular localizations of the DEK1-controlled subnetworks. In the accompanying text box, subnetworks are ranked (1.-4.) according to the percentages of genes with terms affiliated with the respective compartment. **f.** Small network plot depicting the major, significantly enriched inter-subnetwork connections (Pearson residuals > 4; Figure SF4). Drawings of the *Physcomitrella* protonema (c.) and gametophore (d.) stage adapted from Wu et al. 2018. Drawing of a plant cell (e.) adapted from Wikimedia Commons User *Domdomegg*. Subnetwork assignments to developmental stages and cell types (c. and d.) are based on network enrichment of stage-specific DGE sets inferred from *Physcomitrella* gene atlas data (Perroud et al. 2018). Ranked subnetwork assignment of subcellular localizations (e.) is based on ontology enrichment analysis of GO cellular component terms (Figure SF3 and Tables ST3).

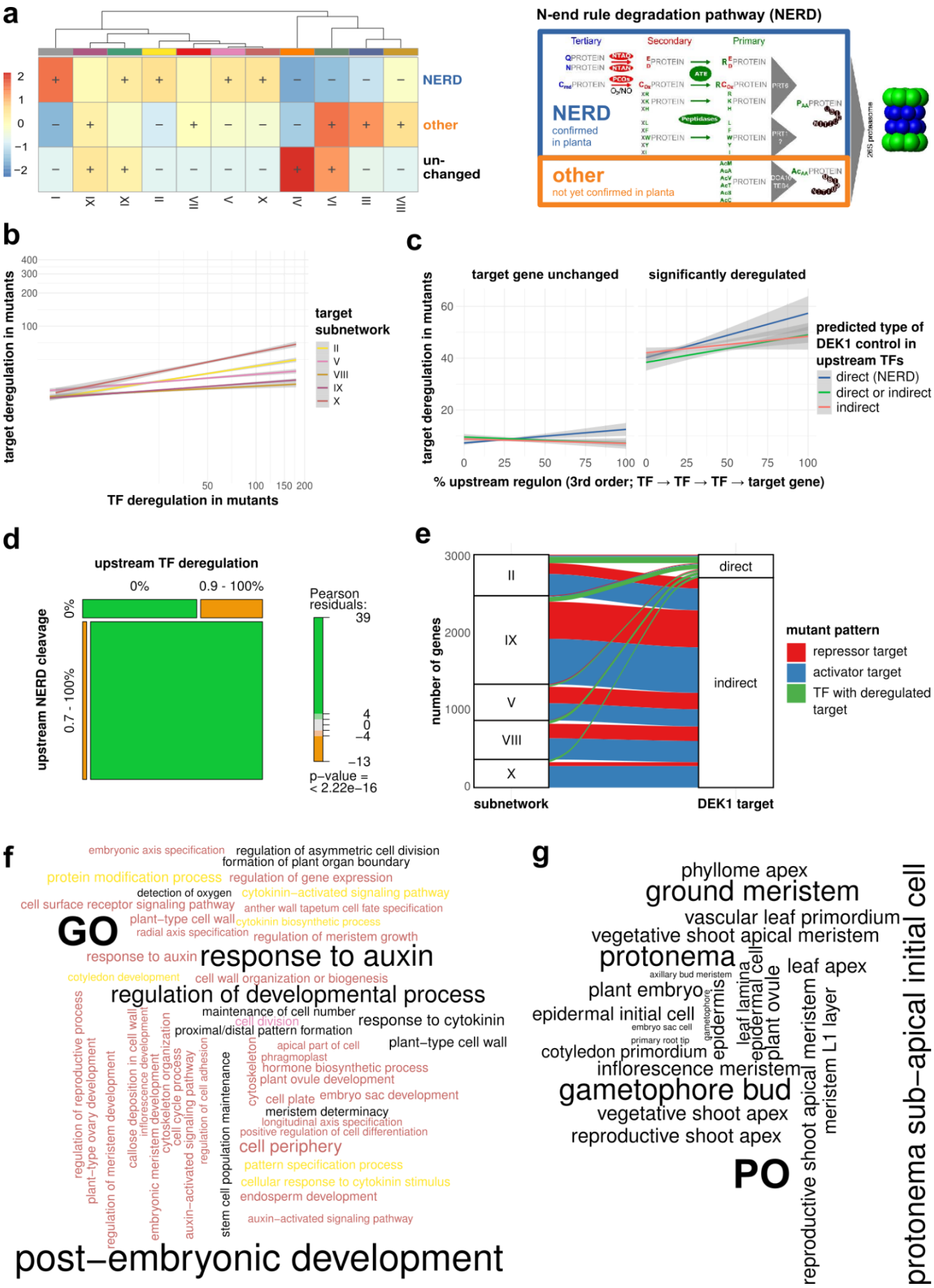
a
NERD
other
un-
changed
N-end rule degradation pathway (NERD)
Tertiary
Secondary
Primary
NERD
confirmed
in planta
other
not yet confirmed in planta
26S proteasome
b
target deregulation in mutants
TF deregulation in mutants
target
subnetwork
II
V
VIII
IX
X
c
target gene unchanged
significantly deregulated
target deregulation in mutants
% upstream regulon (3rd order; TF → TF → TF → target gene)
predicted type of
DEK1 control in
upstream TFs
direct (NERD)
direct or indirect
indirect
d
upstream TF deregulation
0%
0.9 - 100%
upstream NERD cleavage
0.7 - 100%
Pearson
residuals:
39
4
0
−4
−13
p−value =
< 2.22e−16
e
number of genes
subnetwork
DEK1 target
direct
indirect
mutant pattern
repressor target
activator target
TF with deregulated
target
f
GO
post−embryonic development
response to auxin
regulation of developmental process
response to cytokinin
plant−type cell wall
cell periphery
g
PO
protonema
ground meristem
gametophore bud
protonema sub−apical initial cell
phyllome apex
vascular leaf primordium
vegetative shoot apical meristem
leaf apex
plant embryo
epidermal initial cell
cotyledon primordium
inflorescence meristem
vegetative shoot apex
reproductive shoot apex
reproductive shoot apical meristem
meristem L1 layer
epidermis
leaf lamina
epidermal cell
plant ovule

Figure 3. Mutation of DEK1 causes global deregulation of the moss GRN consistent with the pleiotropic phenotype and a post-translational role of the plant calpain in the regulation of protein stability affecting TF↔target interactions a. Network Enrichment Analysis (NEAT) of the prevalence of three specific N-terminal amino acid signature types in predicted calpain cleavage sites of encoded moss proteins. Two of these signature types have been identified in mammals to activate the N-end rule degradation pathway (NERD) resulting in ubiquitylation and subsequent degradation by the 26S proteasome (extended Figure legend on the right adapted from Hoernstein et al., 2016). While the first route has been confirmed to be active in the moss and other plants (NERD), the second route (other) via acetylation of N-terminal residues has not yet been demonstrated *in planta*. The third class represents proteins with no cleavages or sites with N-terminal residues that would not attract the NERD pathway (unchanged). The heatmap depicts the ratio of observed vs expected sizes of specific candidate gene sets encoding for proteins enriched for these types of cleavages among the identified subnetworks. Significant (FDR<0.01) enrichment (+) or depletion (-) is presented by respective cell annotations. Ratios were clustered for rows and columns using the ward.D2 method. **b.** Significant target gene deregulation in DEK1 mutants is positively dependent on deregulation of direct upstream TFs. Linear relationship of target gene and TF deregulation in DEK1 mutants in the five most affected subnetworks. Deregulation of both types of genes is again depicted as the cumulative effect size of the LRTs in each gene. Lines depict the result of generalized linear regression of the cumulative deregulation of TFs (x-axis) and their target genes (y-axis) for each of the five subnetworks. Grey areas depict 95% confidence intervals. **c.** Target gene deregulation displays positive, linear dependency relative to the fraction of directly and indirectly DEK1 calpain-controlled upstream TFs. Linear regression analysis of the cumulative deregulation of target genes (y-axis; sum of LRT effect sizes) and the percentage of the upstream TFs for each gene where TFs are either directly NERD-targeted by DEK1 (blue line; i.e. classified as NERD-type cleavage panel a), indirectly DEK1 targeted (orange line; i.e. significantly deregulated; contained in gene sets displayed in panel b and Fig. 1f) or either of the two types (green line) for unchanged (left plot) and significantly deregulated (right plot; FDR<0.1) target genes. Upstream regulon for each target gene in subnetworks II, V and X was evaluated up to 3rd order relationships. Grey areas depict 95% confidence intervals. **d.** Consistent, DEK1 calpain-dependent deregulation in the three subnetworks implementing the 2D-to-3D transition: The deregulated genes in subnetworks II, V and X display significant enrichment of putative NERD-type calpain cleavages and deregulation of upstream TFs. Mosaic plot depicting the relative proportions of significantly deregulated genes in DEK1 mutants depending on the binary status of their upstream regulon with respect to predicted levels of DEK1 control (x-axis: predicted NERD-type calpain cleavages i.e. direct DEK1 targets; y-axis indirect DEK1 targets). Binary status defines whether the regulon comprises TFs predicted direct (x) or indirect (y) DEK1 targets (>0% of the TFs) or not (=0% TFs). Boxes are colored based on Pearson residuals from a significant χ^2 test of the cross-table comparing the proportions of both binary classes. **e.** Alluvial plot depicting the distribution of the filtered, predicted direct and indirect DEK1 targets among the five predominantly controlled subnetworks. Color-coding of bands reflects directionality of deregulation patterns in the mutant lines (see Fig. 1f for details). The green bands represent unaffected upstream TFs predicted to control the significantly deregulated target genes. **f.** Significantly enriched Gene Ontology (GO) terms associated

with direct and indirect DEK1 target genes are overrepresented with concepts related to observed DEK1 phenotypes in flowering plants and the moss. Word cloud depicting filtered, significantly enriched Gene Ontology (GO) *biological process* and *cellular component* concepts (FDR<0.1). Terms were filtered for overall enriched terms among targets in subnetwork II, V, and X. Furthermore, we curated terms for connection to DEK1 phenotypes. Text size scaled by number of genes per GO term and gene set. Results combined for overall enrichment among DEK1 targets and subnetwork interconnection sets. Color code depicts subnetwork identity of (indirect) target gene. Black indicates overall enrichment among target genes. **g.** Overrepresented tissue and cell type localizations consistent with DEK1 phenotypes and expression patterns. Based on enrichment analysis using Plant Ontology (PO) term annotations for moss genes or their flowering plant orthologs. Word cloud of selected *plant anatomical entity* PO terms displaying an overall enrichment among direct and indirect DEK1 target genes (FDR<0.1). Filtering and selection of terms was carried out as described for GO terms in panel f.

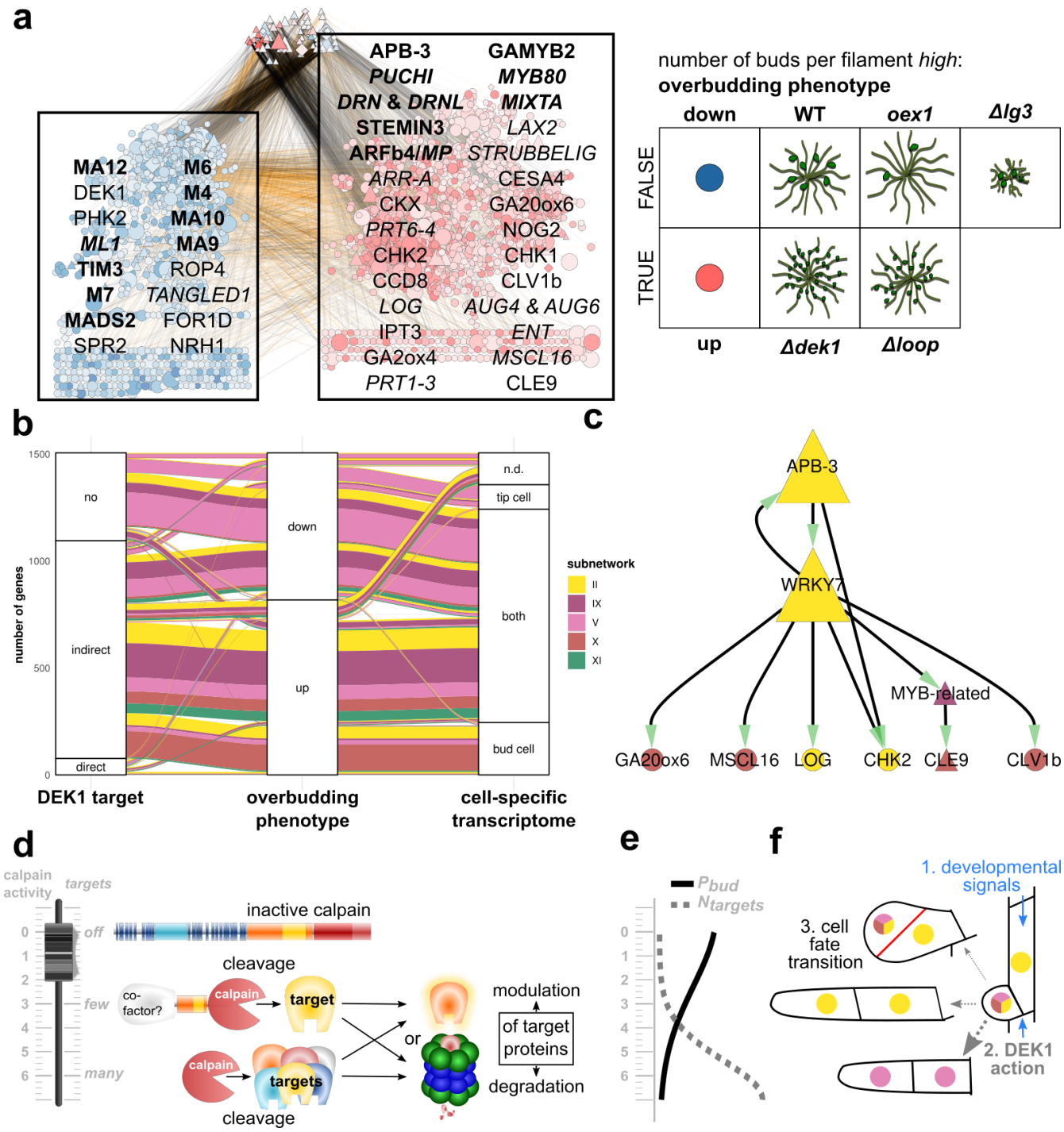

Figure 4. Tracing the mutants' *overbudding* phenotype to deeply conserved, DEK1-guarded, meristematic regulons controlling the 2D-to-3D transition. a. Factorial Differential Gene Expression Network Enrichment Analysis (FDGENEA) of the *overbudding* phenotype reveals enriched subnetworks and upstream regulators associated with high number of buds per filament that comprise key actors in plant meristematic and primordial cell fate control. Network plot of genes with significant association to *overbudding* (left and right node groups in background of overlaid text boxes) and direct, upstream regulators without significant association (top node group). Foreground text boxes display exemplary, predicted DEK1 targets from the *overbudding* up- (right) and down-regulated (left) gene

sets with experimental evidence in flowering plants or the moss. Bold font indicates TFs. Italics is used for names of *Arabidopsis* orthologs. Nodes are color-coded by the kind and strength of a gene's association with the *overbudding* trait (colour intensity gradient relative to log-fold change in DGE analysis; up=positive=red; down=negative=blue). Node sizes relative to the cumulative, absolute deregulation fold-change of the respective gene and any predicted downstream target gene in the mutants. Node shapes: triangles- TFs, diamonds-TRs, inverted triangles-miRNAs, circles- targets. Edge color and intensity: correlation coefficient of connected nodes in DEK1 RNASeq data (black=positive; orange=negative). Panel on the right depicts used genotypes and respective phenotypic character state of the *overbudding* trait (number of buds per filament *high*: FALSE ⇔ TRUE) in wild type and DEK1 mutant lines. **b.** *Overbudding* up-regulated DEK1 targets from subnetworks II and X are enriched in the previously identified bud cell transcriptome (Frank and Scanlon 2015). Alluvial diagram depicting the proportional distribution of subnetworks shared between three categorical sets (from left to right): DEK1 target: predicted direct and indirect DEK1 targets; overbudding phenotype: genes with significant association with the *overbudding* phenotype (up ⇔ down); cell-specific transcriptomics : n.d. not detected; specific to protonemal tip cell; detected but no significant difference between both cell types; specific to gametophore bud cell. Band colouring is based on subnetworks **c.** Key components of the moss CLAVATA peptide (CLE9) and receptor-like kinase (CLV1b) pathway are predicted to be downstream of an *overbudding* up-regulated, DEK1-controlled regulon that comprises a 2D-to-3D master regulator (APB-3) and encodes the integration of several developmental signals (e.g. gibberellin/kaurene (GA20ox6), cytokinin (LOG, CHK2), mechanical stress (MSCL16), peptide (CLE9). Network graph depicting the immediate regulatory context of CLV1b. Full regulatory context is shown in Fig. SF9i. Node sizes are relative to the overall local reaching centrality (fraction of downstream nodes in the global network). Node colouring based on subnetwork affiliation. Triangular nodes are predicted to represent direct cleavage targets of the DEK1 calpain. All predicted regulatory interactions are positive i.e. show positive correlation in wild type and mutants along the RNASeq time course. **d.-f.** Proposed role of DEK1 as a fine-tunable, developmental switch gatekeeping cell fate transitions. Model drawings depicting the proposed relationship between the level of free calpain activity, the number of direct and indirect targets and the developmental consequences in three panels with a shared y-axis (calpain activity). **d.** Model describing three primary DEK1 calpain states (top to bottom): off: immobile, *inactive calpain* in full-length DEK1 protein in plasma membrane. few: mobile, *constrained calpain* - released by auto-catalytic cleavage at several possible locations in the Linker-LG3 domain (Supplementary File). Level of calpain activity, localization, half life and number/kind of targets might be dependent on co-factor interaction. many: mobile, *unconstrained calpain* - pure calpain released by auto-catalytic cleavage directly before or in the CysPc domain. Highest level of calpain activity with a presumably short half life of individual calpain molecules. Potential action as a reset switch resulting in turnover of the entire or large parts of the cells' protein complement. Depending on the exposed N-terminal signatures (Fig. 3a), cleavage of targets by both types of mobile calpain can either result in modulation of the target or degradation by the NERD pathway. **e.** Proposed relationship between the number of DEK1 calpain targets ($N_{targets}$= dashed curve) and the probability of a protonemal cell gaining the bud initial cell fate i.e. gametophore apical stem cell (P_{bud}= solid curve). **f.** Schematic drawing of the cellular fate transitions affected in the *overbudding*

phenotype in three steps. 1. After the perception of developmental signals in the primary filament (blue arrows), a subapical divides and the daughter cell dedifferentiates into a pluripotent, side branch initial. 2. The nature and intensity of the developmental signal (e.g. mechanical stress, phytohormone and peptide gradients) modulates the level of DEK1 action i.e. free calpain activity as indicated in panel **d**. 3. Cell fate transition: The number and kind of DEK1 calpain cleavage targets and impact on protein half live (i.e. NERD) or activation (e.g. CLE peptides) determines one of four outcomes in the following divisions of the side branch initial cell (nuclei are colored by predominant subnetwork): It either differentiates and continues division as a secondary chloronema filament (predominantly subnetwork V; lower two-cells) or a secondary caulonema filament (subnetwork II; middle) or it divides asymmetrically (red cell wall) to form a gametophore bud (top) maintaining a pluripotent gametophore apical stem cell that will give rise to leaf and stem initials (subnetworks V, II, X) and a basal cell (subnetwork II) that will form rhizoid filaments at the base of the gametophore.

References

Ahn, J.W., Kim, M., Lim, J.H., Kim, G.T., Pai, H.S. (2004) Phytocalpain controls the proliferation and differentiation fates of cells in plant organ development. Plant J 38(6), 969-81. 10.1111/j.1365-313X.2004.02102.x.

Amanda, D., Doblin, M.S., Galletti, R., Bacic, A., Ingram, G.C., Johnson, K.L. (2016) DEFECTIVE KERNEL1 (DEK1) Regulates Cell Walls in the Leaf Epidermis. Plant Physiol 172(4), 2204-2218. 10.1104/pp.16.01401.

Amanda, D., Doblin, M.S., Galletti, R., Bacic, A., Ingram, G.C., Johnson, K.L. (2017) Regulation of cell wall genes in response to DEFECTIVE KERNEL1 (DEK1)-induced cell wall changes. Plant Signal Behav 12(8), e1345405. 10.1080/15592324.2017.1345405.

Aoyama, T., Hiwatashi, Y., Shigyo, M., Kofuji, R., Kubo, M., Ito, M., Hasebe, M. (2012) AP2-type transcription factors determine stem cell identity in the moss *Physcomitrella patens*. Development 139(17), 3120-3129. 10.1242/dev.076091.

Araujo, H., Julio, A., Cardoso, M. (2018) Translating genetic, biochemical and structural information to the calpain view of development. Mech Dev 154, 240-250. 10.1016/j.mod.2018.07.011.

Aya, K., Hiwatashi, Y., Kojima, M., Sakakibara, H., Ueguchi-Tanaka, M., Hasebe, M., Matsuoka, M.(2011) The Gibberellin perception system evolved to regulate a pre-existing GAMYB-mediated system during land plant evolution. Nat Commun 2, 544. 10.1038/ncomms1552.

Becraft, P.W., Li, K., Dey, N., Asuncion-Crabb, Y. (2002) The maize dek1 gene functions in embryonic pattern formation and cell fate specification. Development 129(22), 5217-25.

Bolger, A.M., Lohse, M., Usadel, B. (2014) Trimmomatic: a flexible trimmer for Illumina sequence data. Bioinformatics 30(15), 2114-2120. 10.1093/bioinformatics/btu170.

Borghi, L., Kang, J., Ko, D., Lee, Y., Martinoia, E. (2015) The role of ABCG-type ABC transporters in phytohormone transport. Biochem Soc Trans 43(5), 924-30. 10.1042/BST20150106.

Bray, N.L., Pimentel, H., Melsted, P., Pachter, L. (2016) Near-optimal probabilistic RNA-seq quantification. Nat Biotechnol 34(5), 525-527. 10.1038/nbt.3519.

Briesemeister, S., Rahnenführer, J., Kohlbacher, O. (2010) Going from where to why--interpretable prediction of protein subcellular localization. Bioinformatics 26(9), 1232-1238. 10.1093/bioinformatics/btq115.

Cammarata, J., Morales Farfan, C., Scanlon, M., Roeder, A.H.K. (2021) Cytokinin-CLAVATA crosstalk is an ancient mechanism regulating shoot meristem homeostasis in land plants. bioRxiv, 10.1101/2021.08.03.454935

Cardoso, M., Oliveira, D., Araujo, H. (2019) Expression and Activity of Calpain A in Drosophila melanogaster. Methods Mol Biol 1915, 93-101. 10.1007/978-1-4939-8988-1_8.

Casey, M.J., Stumpf, P.S., MacArthur, B.D. (2020) Theory of cell fate. Wiley Interdiscip Rev Syst Biol Med. 12(2), e1471. doi: 10.1002/wsbm.1471.

Chandler, J.W., Werr, W. (2019) DORNRÖSCHEN, DORNRÖSCHEN-LIKE, and PUCHI redundantly control floral meristem identity and organ initiation in Arabidopsis. J Exp Bot 68(13), 3457-3472. 10.1093/jxb/erx208.

Cheng, X., Mwaura, B.W., Chang Stauffer, S.R., Bezanilla, M. (2020) A Fully Functional ROP Fluorescent Fusion Protein Reveals Roles for This GTPase in Subcellular and Tissue-Level Patterning. Plant Cell 32(11), 3436-3451. 10.1105/tpc.20.00440.

Chevalier, D., Batoux, M., Fulton, L., Pfister, K., Yadav, R.K., Schellenberg, M., Schneitz, K. (2005) STRUBBELIG defines a receptor kinase-mediated signaling pathway regulating organ development in Arabidopsis. Proc Natl Acad Sci 102(25), 9074-9079. 10.1073/pnas.0503526102.

Cho, S.H., Coruh, C., Axtell, M.J. (2012) miR156 and miR390 regulate tasiRNA accumulation and developmental timing in *Physcomitrella patens*. Plant Cell 24(12), 4837-49. 10.1105/tpc.112.103176.

Cooper, L., Walls, R.L., Elser, J., Gandolfo, M.A., Stevenson, D.W., Smith, B., Preece, J., Athreya, B., Mungall, C.J., Rensing, S., Hiss, M., Lang, D., Reski, R., Berardini, T.Z., Li, D., Huala, E., Schaeffer, M., Menda, N., Arnaud, E., Shrestha, R., Yamazaki, Y., Jaiswal, P. (2013) The plant ontology as a tool for comparative plant anatomy and genomic analyses. Plant Cell Physiol 54(2), e1. 10.1093/pcp/pcs163.

Cove, D.J., Perroud, P.F., Charron, A.J., McDaniel, S.F., Khandelwal, A., Quatrano R.S. (2009) Culturing the moss *Physcomitrella patens*. Cold Spring Harb Protoc 2009(2), pdb.prot5136. 10.1101/pdb.prot5136.

Demko, V., Perroud, P.F., Johansen, W., Delwiche, Ch.F., Cooper, E., Brown, R.C., Lemmon, B., Remme, P., Ako, E.A., Kugler, K., Mayer, K.F.X., Quatrano, R., Olsen, O.A. (2014) Genetic analysis of DEK1-Loop function in three-dimensional body patterning in *Physcomitrella patens*. Plant Physiol 166(2), 903-91. 10.1104/pp.114.243758.

Eklund, D.M., Svensson, E.M., Kost, B. (2010) *Physcomitrella patens*: a model to investigate the role of RAC/ROP GTPase signalling in tip growth. J Exp Bot 61(7), 1917-37. 10.1093/jxb/erq080.

Emms, D.M., Kelly, S. (2015) OrthoFinder: solving fundamental biases in whole genome comparisons dramatically improves orthogroup inference accuracy. Genome Biol 16(1), 157. 10.1186/s13059-015-0721-2.

Farkas, A., Tompa, P., Schád, E., Sinka, R., Jékely, G., Friedrich, P. (2004) Autolytic activation and localization in Schneider cells (S2) of calpain B from Drosophila**.** Biochem J 378(Pt 2), 299-305. 10.1042/BJ20031310.

Fletcher, J.C., Brand, U., Running, M.P., Simon, R., Meyerowitz, E.M. (1999) Signaling of cell fate decisions by CLAVATA3 in Arabidopsis shoot meristems. Science 283(5409), 1911-4. 10.1126/science.283.5409.1911.

Frank, M.H., Scanlon, M.J. (2015) Cell-specific transcriptomic analyses of three-dimensional shoot development in the moss *Physcomitrella patens*. Plant J 83(4), 743-51. 10.1111/tpj.12928.

Freitas, A.C., Figueiredo, M.J., Campos, E.C., Soave, D.F., Ramos, S.G., Tanowitz, H.B., Celes, M.R. (2016) Activation of Both the Calpain and Ubiquitin-Proteasome Systems Contributes to Septic Cardiomyopathy through Dystrophin Loss/Disruption and mTOR Inhibition. PLoS One 11(11), e0166839. 10.1371/journal.pone.0166839.

Fu, L., Niu, B., Zhu, Z., Wu, S., Li, W. (2012) CD-HIT: accelerated for clustering the next-generation sequencing data. Bioinformatics 28(23), 3150-3152. 10.1093/bioinformatics/bts565.

Galletti, R., Johnson, K.L., Scofield, S., San-Bento, R., Watt, A.M., Murray, J.A., Ingram, G.C. (2015) DEFECTIVE KERNEL 1 promotes and maintains plant epidermal differentiation. Development 142(11), 1978-83. 10.1242/dev.122325.

Gil, D.P., Law, J.N., Murali, T.M. (2017) The PathLinker app: Connect the dots in protein interaction networks. F1000Res 6, 58. 10.12688/f1000research.9909.1.

Graciet, E., Walter, F., Ó'Maoiléidigh, D.S., Pollmann, S., Meyerowitz, E.M., Varshavsky, A., Wellmer, F. (2009) The N-end rule pathway controls multiple functions during Arabidopsis shoot and leaf development. Proc Natl Acad Sci USA 106(32), 13618-23. 10.1073/pnas.0906404106.

Gundu, S., Tabassum, N., Blilou, I. (2020) Moving with purpose and direction: transcription factor movement and cell fate determination revisited. Curr Opin Plant Biol 57, 124-132. 10.1016/j.pbi.2020.08.003.

Harrison, J. (2015) Shooting through time: new insights from transcriptomic data. Trends Plant Sci 20(8), 468-70. 10.1016/j.tplants.2015.06.003

Hata, Y., Kyozuka, J. (2021) Fundamental mechanisms of the stem cell regulation in land plants: lesson from shoot apical cells in bryophytes. Plant Mol Biol Feb 20. 10.1007/s11103-021-01126-y.

Hazak, O., Hardtke, C.S. (2016) CLAVATA 1-type receptors in plant development. J Exp Bot 67(16), 4827-33. 10.1093/jxb/erw247.

Hibara, K., Obara, M., Hayashida, E., Abe, M., Ishimaru, T., Satoh, H., Itoh, J., Nagato, Y. (2009) The ADAXIALIZED LEAF1 gene functions in leaf and embryonic pattern formation in rice. Dev Biol 334(2), 345-54. 10.1016/j.ydbio.2009.07.042

Hirakawa, Y., Uchida, N., Yamaguchi, Y.L., Tabata, R., Ishida, S., Ishizaki, K., Nishihama, R., Kohchi, T., Sawa, S., Bowman, J.L. (2019) Control of proliferation in the haploid meristem by CLE peptide signaling in Marchantia polymorpha. PLoS Genet 15(3), e1007997. 10.1371/journal.pgen.1007997.

Hoernstein, S.N., Mueller, S.J., Fiedler, K., Schuelke, M., Vanselow, J.T., Schuessele, C., Lang, D., Nitschke, R., Igloi, G.L., Schlosser, A., Reski, R. (2016) Identification of Targets and Interaction Partners of Arginyl-tRNA Protein Transferase in the Moss *Physcomitrella patens*. Mol Cell Proteomics 15(6), 1808-22. 10.1074/mcp.M115.057190.

Holdsworth, M.J., Vicente, J., Sharma, G., Abbas, M., Zubrycka, A. (2020) The plant N-degron pathways of ubiquitin-mediated proteolysis. J Integr Plant Biol 62(1), 70-89. 10.1111/jipb.12882.

Horstman, A., Willemsen, V., Boutilier, K., Heidstra, R. (2014) AINTEGUMENTA-LIKE proteins: hubs in a plethora of networks. Trends Plant Sci 19(3), 146-57. 10.1016/j.tplants.2013.10.010.

Huynh-Thu, V.A., Irrthum, A., Wehenkel, L., Geurts, P. (2010) Inferring regulatory networks from expression data using tree-based methods. PLoS One 5(9), e12776. 10.1371/journal.pone.0012776.

Ishikawa, M., Morishita, M., Higuchi, Y., Ichikawa, S., Ishikawa, T., Nishiyama, T., Kabeya, Y., Hiwatashi, Y., Kurata, T., Kubo, M., Shigenobu, S., Tamada, Y., Sato, Y., Hasebe, M. (2019) Physcomitrella STEMIN transcription factor induces stem cell formation with epigenetic reprogramming. Nat Plants 5(7), 681-690. 10.1038/s41477-019-0464-2.

Johansen, W., Ako Eugene, A., Demko, V., Perroud, P.F., Rensing, S., Khaleel Mekhlif, A. Olsen O.A. (2016) The DEK1 calpain Linker functions in three-dimensional body pattering in *Physcomitrella patens*. Plant Physiol 172(2), 1089-1104. 10.1104/pp.16.00925.

Johnson, K.L., Faulkner, C., Jeffree, C.E., Ingram, G.C. (2008) The phytocalpain defective kernel 1 is a novel Arabidopsis growth regulator whose activity is regulated by proteolytic processing. Plant Cell 20(10), 2619-2630. 10.1105/tpc.108.059964.

Johnson, K.L., Degnan, K.A., Ross Walker, J., Ingram, G.C. (2005) AtDEK1 is essential for specification of embryonic epidermal cell fate. Plant J 44(1), 114-127. 10.1111/j.1365-313X.2005.02514.x.

Jones, D.T. (2007) Improving the accuracy of transmembrane protein topology prediction using evolutionary information. Bioinformatics 23(5), 538-544. 0.1093/bioinformatics/btl677.

Jose, J., Ghantasala, S., Choudhury, S.R. (2020) Arabidopsis Transmembrane Receptor-Like Kinases (RLKs): A Bridge between Extracellular Signal and Intracellular Regulatory Machinery. Int J Mol Sci 21(11), 4000. 10.3390/ijms21114000.

de Keijzer, J., Freire Rios, A., Willemsen, V. (2021) *Physcomitrium patens*: A Single Model to Study Oriented Cell Divisions in 1D to 3D Patterning. Int J Mol Sci 22(5), 2626. 10.3390/ijms22052626.

Kirbis, A., Waller, M., Ricca, M., Bont, Z., Neubauer, A., Goffinet, B., Szövényi, P. (2020) Transcriptional Landscapes of Divergent Sporophyte Development in Two Mosses, *Physcomitrium (Physcomitrella) patens* and *Funaria hygrometrica***.** Front Plant Sci 11, 747. 10.3389/fpls.2020.00747.

Kluyver, T., Ragan-Kelley, B., Pérez, F., Granger, B., Bussonnier, M., Frederic, J., Kelley, K., Hamrick, J., Grout, J., Corlay, S., Ivanov, P., Avila, D., Abdalla, S., Willing, C., Jupyter Development Team. (2016) Jupyter Notebooks—a publishing format for reproducible computational workflows. In Proceedings of the 20th International Conference on Electronic Publishing, F. Loizides and B. Schmidt, eds. (IOS Press Ebooks), pp. 87-90. 10.3233/978-1-61499-649-1-87.

Köster, J. and Rahmann, S. (2012) Snakemake—a scalable bioinformatics workflow engine. Bioinformatics 28(19), 2520-2522. 10.1093/bioinformatics/bty350.

Krogh, A., Larsson, B., von Heijne, G., Sonnhammer, E.L. (2001) Predicting transmembrane protein topology with a hidden Markov model: application to complete genomes. J Mol Biol 305(3), 567-580. 10.1006/jmbi.2000.4315.

Kucera, M., Isserlin, R., Arkhangorodsky, A., Bader, G.D. (2016) AutoAnnotate: A Cytoscape app for summarizing networks with semantic annotations. F1000Res 5, 1717. 10.12688/f1000research.9090.1.

Kuroha, T., Tokunaga, H., Kojima, M., Ueda, N., Ishida, T., Nagawa, S., Fukuda, H., Sugimoto, K., Sakakibara, H. (2009) Functional analyses of LONELY GUY cytokinin-activating enzymes reveal the importance of the direct activation pathway in Arabidopsis. Plant Cell 21(10), 3152-3169. 10.1105/tpc.109.068676.

Lang, D., Ullrich, K.K., Murat, F., Fuchs, J., Jenkins J., Haas,. FB., Piednoel M., Gundlach, H., Van Bel, M., Meyberg, R., Vives, C., Morata, J., Symeonidi, A., Hiss, M., Muchero W., Kamisugi, Y., Saleh, O., Blanc, G., Decker, E.L., van Gessel, N., Grimwood, J., Hayes, R.D., Graham, S.W., Gunter, L.E., McDaniel, S.F., Hoernstein, S.N.W., Larsson, A., Li, F.W., Perroud, P.F., Phillips, J., Ranjan, P., Rokshar, D.S., Rothfels, C.J., Schneider, L., Shu, S., Stevenson, D.W., Thümmler, F., Tillich, M., Villarreal Aguilar, J.C., Widiez, T., Wong, G.K., Wymore, A., Zhang, Y., Zimmer, A.D, Quatrano, R.S., Mayer, K.F.X., Goodstein, D., Casacuberta, J.M., Vandepoele, K., Reski, R., Cuming, A.C., Tuskan, G.A., Maumus, F., Salse, J., Schmutz, J., Rensing, S.A. (2018) The *Physcomitrella patens* chromosome-scale assembly reveals moss genome structure and evolution. Plant J 93(3), 515-533. 10.1111/tpj.13801.

Lee, Y.J., Hiwatashi, Y., Hotta, T., Xie, T., Doonan, J.H., Liu, B. (2017) The Mitotic Function of Augmin Is Dependent on Its Microtubule-Associated Protein Subunit EDE1 in *Arabidopsis thaliana*. Curr Biol 27(24), 3891-3897. 10.1016/j.cub.2017.11.030.

Lee, Z.H., Hirakawa, T., Yamaguchi, N., Ito, T. (2019) The Roles of Plant Hormones and Their Interactions with Regulatory Genes in Determining Meristem Activity. Int J Mol Sci 20(16), 4065. 10.3390/ijms20164065.

Leong, S.Y., Yamada, M., Yanagisawa, N., Goshima, G. (2018) SPIRAL2 Stabilises Endoplasmic Microtubule Minus Ends in the Moss *Physcomitrella patens*. Cell Struct Funct 43(1), 53-60. 10.1247/csf.18001.

Lê, S., Josse, J., Husson F. (2008) FactoMineR: An R Package for Multivariate Analysis. J Stat Softw 25(1). 10.18637/jss.v025.i01

Liang, Z., Demko, V., Wilson, R.C., Johnson, K.A., Ahmad, R., Perroud, P.F., Quatrano, R., Zhao, S., Shalchian-Tabrizi, K., Otegui, M.S., Olsen, O.A., Johansen, W. (2013) The catalytic domain CysPc of the DEK1 calpain is functionally conserved in land plants. Plant J 75(5), 742-54. 10.1111/tpj.12235.

Liang, Z., Brown, R.C., Fletcher, J.C., Opsahl-Sorteberg, H.G. (2015) Calpain-Mediated Positional Information Directs Cell Wall Orientation to Sustain Plant Stem Cell Activity, Growth and Development. Plant Cell Physiol 56(9), 1855-1866. 10.1093/pcp/pcv110.

Liaw, A., Wiener, M. (2002) Classification and Regression by randomForest. R News 2(3), 18-22.

Lid, S.E., Gruis, D., Jung, R., Lorentzen, J.A., Ananiev, E., Chamberlin, M., Niu, X., Meeley, R., Nichols, S., Olsen, O.A. (2002) The defective kernel 1 (dek1) gene required for aleurone cell development in the endosperm of maize grains encodes a membrane protein of the calpain gene superfamily. Proc Natl Acad Sci U S A 99(8), 5460-5465. 10.1073/pnas.042098799.

Lid, S.E., Olsen, L., Nestestog, R., Aukerman, M., Brown, R.C., Lemmon, B., Mucha,. M., Opsahl-Sorteberg, H.G, Olsen, OA. (2005) Mutation in the Arabidopisis thaliana DEK1 calpain gene perturbs endosperm and embryo development while over-expression affects organ development globally. Planta 221(3), 339-351. 10.1007/s00425-004-1448-6.

Lindner, A.C., Lang, D., Seifert, M., Podlešáková, K., Novák, O., Strnad, M., Reski, R., von Schwartzenberg, K. (2014) Isopentenyltransferase-1 (IPT1) knockout in Physcomitrella together with phylogenetic analyses of IPTs provide insights into evolution of plant cytokinin biosynthesis. J Exp Bot 65(9), 2533-2543. 10.1093/jxb/eru142.

Liu, Z., Cao, J., Gao, X., Ma, Q., Ren, J., Xue, Y. (2011) GPS-CCD: a novel computational program for the prediction of calpain cleavage sites. PLoS One 6(4), e19001. 10.1371/journal.pone.0019001.

Majovsky, P., Naumann, C., Lee, C.W., Lassowskat, I., Trujillo, M., Dissmeyer, N., Hoehenwarter, W. (2014) Targeted proteomics analysis of protein degradation in plant signaling on an LTQ-Orbitrap mass spectrometer**.** J Proteome Res. 13(10), 4246-4258. 10.1021/pr500164j.

Martinez, P., Dixit, R., Balkunde, R.S., Zhang, A., O'Leary, S.E., Brakke, K.A., Rasmussen, C.G. (2020) TANGLED1 mediates microtubule interactions that may promote division plane positioning in maize. J Cell Biol 219(8), e201907184. 10.1083/jcb.201907184.

Miyazaki, T., Tonami, K., Hata, S., Aiuchi, T., Ohnishi, K., Lei, X.F., Kim-Kaneyama, J.R., Takeya, M., Itabe, H., Sorimachi, H., Kurihara, H., Miyazaki, A. (2016) Calpain-6 confers atherogenicity to macrophages by dysregulating pre-mRNA splicing. J Clin Invest 126(9), 3417-3432. 10.1172/JCI85880.

Miyazaki, S., Hara, M., Ito, S., Tanaka, K., Asami, T., Hayashi, K.I., Kawaide, H., Nakajima, M. (2018) An Ancestral Gibberellin in a Moss *Physcomitrella patens*. Mol Plant 11(8), 1097-1100. 10.1016/j.molp.2018.03.010.

Moldoveanu, T., Hosfield, C.M., Lim, D., Elce, J.S., Jia, Z., Davies, P.L. (2002) A Ca(2+) switch aligns the active site of calpain. Cell 108(5), 649-660. 10.1016/s0092-8674(02)00659-1.

Moody, L.A., Kelly, S., Rabbinowitsch, E., Langdale, J.A. (2018) Genetic Regulation of the 2D to 3D Growth Transition in the Moss *Physcomitrella patens*. Curr Biol 28(3), 473-478.e5. 10.1016/j.cub.2017.12.052.

Moody, L.A. (2019) The 2D to 3D growth transition in the moss *Physcomitrella patens*. Curr Opin Plant Biol 47, 88-95. 10.1016/j.pbi.2018.10.001.

Moody, L.A., Kelly, S., Clayton, R., Weeks, Z., Emms, D.M., Langdale, J.A. (2021) NO GAMETOPHORES 2 Is a Novel Regulator of the 2D to 3D Growth Transition in the Moss *Physcomitrella patens*. Curr Biol 31(3), 555-563.e4. 10.1016/j.cub.2020.10.077.

Mot, A., Prell, E., Klecker, M., Naumann, Ch., Faden, F., Westermann, B., Dissmeyer, N. (2017). Real-time detection of N-end rule-mediated ubiquitination via fluorescently labeled substrate probes. New Phytol 217(2), 613-624. 10.1111/nph.14497.

Muñoz-Nortes, T., Wilson-Sánchez, D., Candela, H., Micol, J.L. (2014) Symmetry, asymmetry, and the cell cycle in plants: known knowns and some known unknowns. J Exp Bot 65(10), 2645-2655. 10.1093/jxb/ert476.

Nakagami, H., Sugiyama, N., Mochida, K., Daudi, A., Yoshida, Y., Toyoda, T., Tomita, M., Ishihama, Y., Shirasu, K. (2010) Large-scale comparative phosphoproteomics identifies conserved phosphorylation sites in plants. Plant Physiol 153(3), 1161-1174. 10.1104/pp.110.157347.

Nguyen, K.T., Mun, S.H., Lee, C.S., Hwang, C.S. (2018) Control of protein degradation by N-terminal acetylation and the N-end rule pathway. Exp Mol Med 50(7), 1-8. 10.1038/s12276-018-0097-y.

Nühse, T.S., Stensballe, A., Jensen, O.N., Peck, S.C. (2004) Phosphoproteomics of the Arabidopsis plasma membrane and a new phosphorylation site database. Plant Cell 16(9), 2394-405. 10.1105/tpc.104.023150.

Oliver, W.T., Keel, B.N., Lindholm-Perry, A.K., Horodyska, J., Foote, A.P. (2018) The effects of Capn1 gene inactivation on the differential expression of genes in skeletal muscle. Gene 668, 54-58. 10.1016/j.gene.2018.05.040.

Olsen, O.A., Perroud, P.F., Johansen, W., Demko, V. (2015) DEK1; missing piece in puzzle of plant development. Trends Plant Sci 20(2), 70-71. 10.1016/j.tplants.2015.01.003.

Olsen, O.A. (2020) The Modular Control of Cereal Endosperm Development. Trends Plant Sci 25(3), 279-290. 10.1016/j.tplants.2019.12.003.

Ono, Y., Sorimachi, H. (2012) Calpains: an elaborate proteolytic system. Biochim Biophys Acta 1824(1), 224-236. 10.1016/j.bbapap.2011.08.005.

Ono, Y., Saido, T.C., Sorimachi, H. (2016) Calpain research for drug discovery: challenges and potential. Nat Rev Drug Discov 15(12), 854-876. 10.1038/nrd.2016.212.

Oshima, Y., Shikata, M., Koyama, T., Ohtsubo, N., Mitsuda, N., Ohme-Takagi, M. (2013) MIXTA-like transcription factors and WAX INDUCER1/SHINE1 coordinately regulate cuticle development in Arabidopsis and Torenia fournieri. Plant Cell 25(5), 1609-1624. 10.1105/tpc.113.110783.

Panteris, E., Kouskouveli, A., Pappas, D., Adamakis, I.S. (2021) Cytokinesis in fra2 *Arabidopsis thaliana* p60-Katanin Mutant: Defects in Cell Plate/Daughter Wall Formation. Int J Mol Sci 22(3), 1405. 10.3390/ijms22031405.

Park, C.Y., Lee, J.H., Yoo, J.H., Moon, B.C., Choi, M.S., Kang, Y.H., Lee, S.M., Kim, H.S., Kang, K.Y., Chung, W.S., Lim, C.O., Cho, M.J. (2005) WRKY group IId transcription factors interact with calmodulin. FEBS Lett 579(6), 1545-1550. 10.1016/j.febslet.2005.01.057.

Perroud, P.F., Demko, V., Johansen, W., Wilson, R.C., Olsen, O.A., Quatrano, R.S. (2014) Defective Kernel 1 (DEK1) is required for three-dimensional growth in *Physcomitrella patens*. New Phytol 203(3), 794-804. 10.1111/nph.12844.

Perroud, P.F., Haas, F.B., Hiss, M., Ullrich, K.K., Alboresi, A., Amirebrahimi, M., Barry, K., Bassi, R., Bonhomme, S., Chen, H., Coates, J.C., Fujita, T., Guyon-Debast, A., Lang, D., Lin, J., Lipzen, A., Nogué, F., Oliver, M.J., Ponce de León, I., Quatrano, R.S., Rameau, C., Reiss, B., Reski, R., Ricca, M., Saidi, Y., Sun, N., Szövényi, P., Sreedasyam, A., Grimwood, J., Stacey, G., Schmutz, J., Rensing, S.A. (2018) The *Physcomitrella patens* gene atlas project: large-scale RNA-seq based expression data. Plant J 95(1), 168-182. 10.1111/tpj.13940

Perroud, P.F., Meyberg, R., Demko, V., Quatrano, R.S., Olsen, O.A., Rensing, S.A. (2020) DEK1 displays a strong subcellular polarity during *Physcomitrella patens* 3D growth. New Phytol 226(4), 1029-1041. 10.1111/nph.16417.

Pertea, G., Pertea, M. (2020) GFF Utilities: GffRead and GffCompare. F1000Res 28(9), ISCB Comm J-304. 10.12688/f1000research.23297.2.

Piatkov, K.I., Oh, J.H., Liu, Y., Varshavsky, A. (2014) Calpain-generated natural protein fragments as short-lived substrates of the N-end rule pathway. Proc Natl Acad Sci USA 111(9), E817-826. 10.1073/pnas.1401639111.

Pierre-Jerome, E., Drapek, C., Benfey, P.N. (2018) Regulation of division and differentiation of plant stem cells. Annu Rev Cell Dev Biol 34, 289-310. 10.1146/annurev-cellbio-100617-062459.

Pimentel, H., Bray, N.L., Puente, S., Melsted, P., Pachter, L. (2017) Differential analysis of RNA-seq incorporating quantification uncertainty. Nat Methods 14(7), 687-690. 10.1038/nmeth.4324.

Proust, H., Hoffmann, B., Xie, X., Yoneyama, K., Schaefer, D.G., Yoneyama, K., Nogué, F., Rameau, C. (2011) Strigolactones regulate protonema branching and act as a quorum sensing-like signal in the moss *Physcomitrella patens*. Development 138(8), 1531-1539. 10.1242/dev.058495.

Ramírez-González, R.H., Borrill, P., Lang, D., Harrington, S.A., Brinton, J., Venturini, L., Davey, M., Jacobs, J., van Ex, F., Pasha, A., Khedikar, Y., Robinson, S.J., Cory, A.T., Florio, T., Concia, L., Juery, C., Schoonbeek, H., Steuernagel, B., Xiang, D., Ridout, C.J., Chalhoub, B., Mayer, K.F.X., Benhamed, M., Latrasse, D., Bendahmane, A., International Wheat Genome Sequencing Consortium, Wulff BBH, Appels, R., Tiwari, V., Datla, R., Choulet, F., Pozniak, C.J., Provart, N.J., Sharpe, A.G., Paux, E., Spannagl, M., Bräutigam, A., Uauy, C. (2018) The transcriptional landscape of polyploid wheat. Science 361(6403), eaar6089. 10.1126/science.aar6089.

Rensing, S.A., Goffinet, B., Meyberg, R., Wu, S.Z., Bezanilla, M. (2020) The moss *Physcomitrium* (*Physcomitrella*) *patens*: A model organism for non-seed plants. Plant Cell 32(5), 1361-1376. 10.1105/tpc.19.00828.

Ryo, M., Yamashino, T., Nomoto, Y., Goto, Y., Ichinose, M., Sato, K., Sugita, M., Aoki, S. (2018) Light-regulated PAS-containing histidine kinases delay gametophore formation in the moss *Physcomitrella patens*. J Exp Bot 69(20), 4839-4851. 10.1093/jxb/ery257.

Shinkai-Ouchi, F., Koyama, S., Ono, Y., Hata, S., Ojima, K., Shindo, M., duVerle, D., Ueno, M., Kitamura, F., Doi, N., Takigawa, I., Mamitsuka, H., Sorimachi, H. (2016) Predictions of cleavability of calpain proteolysis by quantitative structure-activity relationship analysis using newly determined cleavage sites and catalytic efficiencies of an oligopeptide array.
Mol Cell Proteomics 15(4), 1262-1280. 10.1074/mcp.M115.053413.

Schulz, P., Reski, R., Maldiney, R., Laloue, M., von Schwartzenberg, K. (2000) Kinetics of cytokinin production and bud formation in Physcomitrella*:* Analysis of wild type, a developmental mutant and two of its *ipt* transgenics. J Plant Physiol 156(5-6), 768-774. 10.1016/S0176-1617(00)80246-1.

Schuessele, C., Hoernstein, S.N., Mueller, S.J., Rodriguez-Franco, M., Lorenz, T., Lang, D., Igloi, G.L., Reski, R. (2016) Spatio-temporal patterning of arginyl-tRNA protein transferase (ATE) contributes to gametophytic development in a moss. New Phytol 209(3), 1014-1027. 10.1111/nph.13656.

Schwartzenberg, K., Núñez, M.F., Blaschke, H., Dobrev, P.I., Novák, O., Motyka, V., Strnad, M. (2007) Cytokinins in the bryophyte *Physcomitrella patens*: analyses of activity, distribution, and cytokinin oxidase/dehydrogenase overexpression reveal the role of extracellular cytokinins. Plant Physiol 145(3), 786-800. 10.1104/pp.107.103176.

Schwartzenberg, K., Lindner, A.C., Gruhn, N., Šimura, J., Novák, O., Strnad, M., Gonneau, M., Nogué, F., Heyl, A. (2016) CHASE domain-containing receptors play an essential role in the cytokinin response of the moss *Physcomitrella patens*. J Exp Bot 67(3), 667-679.

Scrucca, L., Fop, M., Murphy T.B., Raftery, A.E. (2016) mclust 5: Clustering, Classification and Density Estimation Using Gaussian Finite Mixture Models. R J 8(1), 289-317. 10.32614/RJ-2016-021.

Shannon, P., Markiel, A., Ozier, O., Baliga, N.S., Wang, J.T., Ramage, D., Amin, N., Schwikowski, B., Ideker, T. (2003) Cytoscape: a software environment for integrated models of biomolecular interaction networks. Genome Res 13(11), 2498-2504. 10.1101/gr.1239303.

Shao, W., Dong, J. (2016) Polarity in plant asymmetric cell division: Division orientation and cell fate differentiation. Dev Biol 419(1), 121-131. 10.1093/jxb/erv479.

Signorelli, M., Vinciotti, V., Wit, E.C. (2016) NEAT: an efficient network enrichment analysis test. MBC Bioinformatics 17(1), 352. 10.1186/s12859-016-1203-6.

Sorimachi, H., Ono, Y. (2012) Regulation and physiological roles of the calpain system in muscular disorders. Cardiovasc Res 96(1), 11-22. 10.1093/cvr/cvs157.

Spinozzi, S., Albini, S., Best, H., Richard, I. (2021) Calpains for dummies: What you need to know about the calpain family. Biochim Biophys Acta Proteins Proteom 1869(5), 140616. 10.1016/j.bbapap.2021.140616.

Staudt, Ch.L., Sazonovs, A., Meyerhenke, H. (2016) NetworKit: A tool suite for large-scale complex network analysis. Network Science 4 (4), 508-530. 10.1017/nws.2016.20

Storr, S.J., Carragher, N.O., Frame, M.C., Parr ,T., Martin, S.G. (2011) The calpain system and cancer. Nat Rev Cancer 11(5), 364-374. 10.1038/nrc3050.

Swarup, R., Bhosale, R. (2019) Developmental roles of AUX1/LAX auxin influx carriers in plants. Front Plant Sci 10, 1306. 10.3389/fpls.2019.01306.

Takada, S., Iida, H. (2014) Specification of epidermal cell fate in plant shoots. Front Plant Sci 5, 49. 10.3389/fpls.2014.00049

Tang, H., Duijts, K., Bezanilla, M., Scheres, B., Vermeer, J.E.M., Willemsen, V. (2020) Geometric cues forecast the switch from two- to three-dimensional growth in *Physcomitrella patens*. New Phytol 225(5), 1945-1955. 10.1111/nph.16276.

The Gene Ontology Consortium. (2017) Expansion of the Gene Ontology knowledgebase and resources. Nucleic Acids Res 45(D1), D331-D338. 10.1093/nar/gkw1108.

Tian, Q., Olsen, L., Sun, B., Lid, S.E., Brown, R.C., Lemmon, B.E., Fosnes, K., Gruis, D.F., Opsahl-Sorteberg, H.G., Otegui, M.S., Olsen, O.A. (2007) Subcellular localization and functional domain studies of DEFECTIVE KERNEL1 in maize and Arabidopsis suggest a model for aleurone cell fate specification involving CRINKLY4 and SUPERNUMERARY ALEURONE LAYER1. Plant Cell 19(10), 3127-3145. 10.1105/tpc.106.048868.

Tian, X., Inoue, K., Zhang, Y., Wang, Y., Sperati, C.J., Pedigo, C.E., Zhao, T., Yan, M., Groener, M., Moledina, D.G., Ebenezer, K., Li, W., Zhang, Z., Liebermann, D.A., Greene, L., Greer, P., Parikh, C.R., Ishibe, S. (2020) Inhibiting calpain 1 and 2 in cyclin G associated kinase-knockout mice mitigates podocyte injury. JCI Insight 5(22), e142740. 10.1172/jci.insight.142740.

To, J.P., Kieber, J.J. (2008) Cytokinin signaling: two-components and more. Trends Plant Sci 13(2), 85-92. 10.1016/j.tplants.2007.11.005.

Tran, D., Galletti, R., Neumann, E.D., Dubois, A., Sharif-Naeini, R., Geitmann, A., Frachisse, J.M., Hamant, O., Ingram, G.C. (2017) A mechanosensitive Ca^{2+} channel activity is dependent on the developmental regulator DEK1. Nat Commun 18(1), 1009. 10.1038/s41467-017-00878-w.

Varshavsky, A. (2012) Three decades of studies to understand the functions of the ubiquitin family. Methods Mol Biol 832, 1-11. 10.1007/978-1-61779-474-2_1.

Nemec Venza, Z., Madden, C., Stewart, A., Liu, W., Novák, O., Pěnčík, A., Cuming, A.C., Kamisugi, Y., Jill Harrison, C. (2021). PpRPK2 modulates auxin homeostasis and transport to specify stem cell identity and plant shape in the moss Physcomitrella. bioRxiv, 10.1101/2021.06.24.449551

Vidali, L., van Gisbergen, P.A., Guérin, C., Franco, P., Li, M., Burkart, G.M., Augustine, R.C., Blanchoin, L., Bezanilla, M. (2009) Rapid formin-mediated actin-filament elongation is essential for polarized plant cell growth. Proc Natl Acad Sci USA 106(32), 13341-13346. 10.1073/pnas.0901170106.

Vieira, V., Cardoso, M.A., Araujo, H. (2017) Calpain A controls mitotic synchrony in the Drosophila blastoderm embryo. Mech Dev 144(Pt B), 141-149. 10.1016/j.mod.2016.05.005.

Wang, C., Barry, J.K., Min, Z., Tordsen, G., Rao, A.G., Olsen, O.A. (2003) The calpain domain of the maize DEK1 protein contains the conserved catalytic triad and functions as a cysteine proteinase. J Biol Chem 278(36), 34467-34474. 10.1074/jbc.M300745200.

Warnes, G.R., Bolker, B., Lumley, T., Johnson, R.C. (2018) Contributions from Randall C. Johnson are Copyright SAIC-Frederick, Inc. Funded by the Intramural Research Program, of the NIH, National Cancer Institute and Center for Cancer Research under NCI Contract NO1-CO-12400. (2018) gmodels: Various R Programming Tools for Model Fitting. R package version 2.18.1.

Whitewoods, C.D., Cammarata, J., Nemec Venza, Z., Sang, S., Crook, A.D., Aoyama, T., Wang, X.Y., Waller, M., Kamisugi, Y., Cuming, A.C., Szövényi, P., Nimchuk, Z.L., Roeder, A.H.K., Scanlon, M.J., Harrison, C.J. (2018) CLAVATA was a genetic novelty for the morphological innovation of 3D growth in land plants. Curr Biol 28(15), 2365-2376. 10.1016/j.cub.2018.05.068.

Wilson, M.E., Maksaev, G., Haswell, E.S. (2013) MscS-like mechanosensitive channels in plants and microbes. Biochemistry 52(34), 5708-5722. 10.1021/bi400804z.

Wu, S.Z., Yamada, M., Mallett, D.R., Bezanilla, M. (2018) Cytoskeletal discoveries in the plant lineage using the moss *Physcomitrella patens*. Biophys Rev 10(6), 1683-1693. 10.1007/s12551-018-0470-z.

Xu, Y., Iacuone, S., Li, S.F., Parish, R.W. (2014) MYB80 homologues in Arabidopsis, cotton and Brassica: regulation and functional conservation in tapetal and pollen development. BMC Plant Biol 14, 278. 10.1186/s12870-014-0278-3.

Yamaguchi, Y.L., Ishida, T., Sawa, S. (2016) CLE peptides and their signaling pathways in plant development. J Exp Bot 67(16), 4813-4826. 10.1093/jxb/erw208.

Zhao, S., Liang, Z., Demko, V., Wilson, R., Johansen, W., Olsen, O.A., Shalchian-Tabrizi, K. (2012) Massive expansion of the calpain gene family in unicellular eukaryotes. BMC Evol Biol 12, 193. 10.1186/1471-2148-12-193.

Zimmer, A.D., Lang, D., Buchta, K., Rombauts, S., Nishiyama, T., Hasebe, M., Van de Peer, Y., Rensing, S.A., Reski, R. (2013) Reannotation and extended community resources for the genome of the non-seed plant *Physcomitrella patens* provide insights into the evolution of plant gene structures and functions. BMC Genomics 14, 498. 10.1186/1471-2164-14-498.